NATIONAL ADVISORY COMMITTEE FOR AERONAUTICS

TECHNICAL MEMORANDUM

No. 1208

CALCULATION OF COUNTERROTATING PROPELLERS

By F. Ginzel

Translation of Forschungsbericht Nr. 1752, January 1943

Washington

March 1949

NATIONAL ADVISORY COMMITTEE FOR AERONAUTICS

TECHNICAL MEMORANDUM No. 1208

CALCULATION OF COUNTERROTATING PROPELLERS*

By F. Ginzel

Abstract: A method for calculation of a counterrotating propeller which is similar to Walchner's method for calculation of the single propeller in the free air stream is developed and compared with measurements. Several dimensions which are important for the design are given and simple formulas for the gain in efficiency derived. Finally a survey of the behavior of the propeller for various operating conditions is presented.

Outline:

---

* "Zur Berechnung von Gegenlaufschrauben." Zentrale für wissenschaftliches Berichtswesen der Luftfahrtforschung des Generalluftzeugmeisters (ZWB) Berlin-Adlershof, Forschungsbericht Nr. 1752, Jan. 25, 1943.

I. SYMBOLS

A lift

c_a lift coefficient $\left(c_a = \frac{dA}{\frac{\rho}{2} W_w^2 z l \, dr}\right)$

c_l power loading $\left(c_l = \frac{N}{\frac{\rho}{2} F_p v^3}\right)$

c_s thrust loading $\left(c_s = \frac{S}{\frac{\rho}{2} F_p v^2}\right)$

d thickness of the profile

F_p propeller disk area

k_l power coefficient $\left(k_l = \frac{N}{\frac{\rho}{2} F_p U^3}\right)$

k_s thrust coefficient $\left(k_s = \frac{S}{\frac{\rho}{2} F_p U^2}\right)$

l wing chord (width of the blade)

N power of rotation

R radius of the propeller

r	radius of a section, profile
S	thrust for undisturbed free-stream conditions
U	peripheral speed of the propeller $(U = \omega R)$
v	rate of advance, W top velocity $\left(W = \sqrt{v^2 + U^2}\right)$
w	profile velocity $\left(w = \sqrt{v^2 + (r\omega)^2}\right)$
w_w	effective profile velocity
$\frac{w_a}{2}$	axial induced velocity
$\frac{w_n}{2}$	induced velocity
$\frac{w_t}{2}$	tangential induced velocity
x	radius nondimensional $\left(x = \frac{r}{R}\right)$
z	number of blades
α_d	angle of attack, pressure side
α_i	induced angle
β	blade angle
β_d	blade angle, pressure side
ϵ_p	efficiency of the blade element $\epsilon_p = \tan \gamma$ (profile drag-lift coefficient)
η_a	axial efficiency
η_i	ideal efficiency
λ	ratio of advance
ρ	density of air
φ	angle of advance

φ_w effective angle of advance

ω angular velocity

Special symbols in this treatise:

Index I refers to the front propeller, index II to the rear propeller

Index g refers to the counterrotating propeller

Index e refers to the single propeller

Dimensions with + contain the influence of the other partner upon the propeller under consideration (See fig. 5.)

$\bar{v}_1 = 1 + \kappa_I \frac{\overline{w_{aI}}}{2} + \frac{\overline{w_{aII}}}{2} \approx 1 + \kappa_{II} \frac{\overline{w_{aII}}}{2} + \frac{\overline{w_{aI}}}{2}$ axial velocity at the propeller disk.

II. INTRODUCTION

The decrease in efficiency for high flight velocities is due mainly to rotational losses. (See fig. 1, which corresponds to a figure from [2][1]). The counterrotating propeller makes a partial recovery of these losses possible. The elimination of the free propeller moment (rolling moment) and the possibility of higher power absorption for the same diameter are further advantages. The arrangement of the two propellers on one axis offers advantages for flight behavior even for extreme operating conditions, for instance, a propeller acting as a brake. Therefore, below an arrangement for counterrotation is investigated in which both partners are arranged one closely behind the other on the same axis and have the same number and shape of blades, the same diameter and equal and opposite angular speed, but a different distribution of the blade angle over the radius. The investigations are performed principally at the blade cross section so that no presumption is made about the distribution of the circulation over the radius: Therein lies an advantage because the blade for optimum distribution resulting from aerodynamic considerations cannot be constructed; the practice, therefore, must reach a compromise which cannot form the basis of an aerodynamic investigation.

---

[1]The numbers in brackets refer to the references at the end of this report.

III. BASES FOR CALCULATION

1. Bases for Calculation of the Single Propeller in the Free Air Stream

We recapitulate in this section at first the course of a usual propeller calculation (according to [14]) in order to see clearly, in the next section, whether additional neglections, and if so, of what kind, enter into the calculation of the counterrotating propeller and how the formulas of the single propeller must be extended to cover the mutual influence of the two partners.

The circulation Γ around all z blades of the propeller at the section r equals the line integral over the differences $\tilde{w}_t$ of the tangential velocities ahead of and behind the propeller (see fig. 3) along the circle of the radius r in the fully developed slipstream (ultimate wake)

$$z\Gamma = \int_0^{2\pi} \tilde{w}_t r \, d\vartheta \tag{1}$$

If we define the mean value factor κ by

$$\frac{1}{2\pi}\int_0^{2\pi} \tilde{w}_t \, d\vartheta = \kappa w_t \tag{2}$$

where w_t is the maximum $\tilde{w}_t$ which is reached at the location of a propeller vortex in the projection of a blade, we can substitute for (1) the notation

$$z\Gamma = 2r\pi\kappa w_t \tag{3}$$

If we call the true free stream velocity at the location of a blade element and relative to it w_w, the Kutta-Joukowsky condition for the lift element dA in frictionless flow and the defining equation for the lift coefficient c_a supply the following relation between

c_a and Γ or between c_a and w_t

$$dA = \rho z \Gamma w_w \, dr = \rho 2r\pi\kappa w_t w_w \, dr = \frac{\rho}{2} w_w^2 c_a z \, l \, dr \tag{4}$$

or

$$c_a = \frac{4r\pi\kappa}{zl} \frac{w_t}{w_w} \tag{5}$$

with l representing the chord of the profile at the section r.

Figure 2 is the usual diagram of velocities and forces for the blade element. The figure, in particular, the marked right angle between w_w and $\frac{w_n}{2}$, is valid for small loads. Jet contraction and reduced pressure in the slipstream are neglected. Taking the right angle mentioned above into consideration we obtain

$$\frac{w_t}{w_w} = 2 \sin \varphi_w \tan \alpha_i$$

with φ_w representing the effective angle of advance and α_i the induced angle of attack. Then there follows for the lift coefficient from (5)

$$c_a = \frac{8x}{\frac{z}{\pi}\frac{l}{R}} \kappa \sin \varphi_w \tan \alpha_i = \frac{8x}{\frac{z}{\pi}\frac{l}{R}} \kappa \sin \left(\beta_d - \alpha_d\right) \tan \left(\beta_d - \varphi - \alpha_d\right) \tag{6}$$

Only c_a and the angle of attack α_d which is referred to the pressure side are unknown in this equation (excepting the mean value factor κ), for the blade angle β_d, the angle of advance φ, the propeller radius R and the ratio $x = \frac{r}{R}$ are given. As in the wing theory the relation between c_a and α_d which is known from the profile measurements or from the plane theory is used for determining these two quantities.

For calculation of the characteristic values of the propeller we now designate the peripheral speed $R\omega$ as U, the rate of advance $\frac{v}{U}$ as λ and take from figure 2

$$w_w = \frac{r\omega}{\cos \varphi} \cos \alpha_i = Ux \frac{\cos \alpha_i}{\cos \varphi} = U \cos \alpha_i \sqrt{x^2 + \lambda^2}$$

The propeller disk area $R^2\pi$ is designated F_p, and there follows from (4)

$$\frac{dA}{\frac{\rho}{2} U^2 F_p} = \frac{z}{\pi} \frac{l}{R} \left(x^2 + \lambda^2\right) c_a \cos^2 \alpha_i dx \tag{7}$$

The considerations so far were valid for flows without losses. Because of the actually always existing flow losses the air force changes by the drag component

$$dW = d\,A\epsilon_p$$

$\epsilon_p = \tan \gamma$ is the efficiency of the blade element which is to be taken from profile measurements at the respective Reynolds number so that one obtains for the thrust force dS and for the tangential force dT:

$$dS = dA \cos\left(\varphi_w + \gamma\right) / \cos \gamma$$

$$dT = dA \sin \left(\varphi_w + \gamma\right) / \cos \gamma = dS \tan \left(\varphi_w + \gamma\right)$$

With (6) the result for the thrust coefficient is $k_s = \frac{S}{\frac{\rho}{2} F_p U^2}$

and for the power coefficient $k_l = \frac{N}{\frac{\rho}{2} F_p U^3} = \frac{TR\omega}{\frac{\rho}{2} F_p U^3}$

$$\frac{dk_s}{dx} = \frac{z}{\pi}\frac{l}{R}\left(x^2 + \lambda^2\right)c_a \cos^2\alpha_1 \cos\left(\varphi_w + \gamma\right)/\cos\gamma \qquad (8)$$

$$\frac{dk_l}{dx} = \frac{dk_s}{dx}\, x \tan\left(\varphi_w + \gamma\right) \qquad (9)$$

The formulas (3) to (9) are sufficient for calculation of the single propeller. We shall indicate several further relations which will be useful for calculation of the counterrotating propeller. The frictionless thrust element can be inferred from the circulation (3) by means of the Kutta-Joukowsky condition to be

$$dS = \rho\left(r\omega - \frac{w_t}{2}\right)2r\pi\kappa w_t\, dr$$

If we introduce by division of all velocities with the flight velocity v nondimensional velocities and mark them with bars, and if we further designate the local (referred to the local area element) coefficients $\frac{dc}{d(x^2)}$ abbreviatedly as c', another notation may be used for the local thrust loading $\left(c_s = \frac{S}{\frac{\rho}{2}F_p v^2}\right)$:

$$c_s' = 2\kappa\bar{w}_t\left(\bar{r}\bar{\omega} - \frac{\bar{w}_t}{2}\right) \qquad (10)$$

Likewise there follows from the power element

$$r\omega\, dT = r\omega\rho\left(v + \frac{w_a}{2}\right)2r\pi\kappa w_t\, dr$$

for the local power loading $\left(c_l = \frac{N}{\frac{\rho}{2}F_p v^3}\right)$

$$c_l' = 2\bar{r}\bar{\omega}\kappa\bar{w}_t\left(1 + \frac{\bar{w}_a}{2}\right) \qquad (11)$$

The equations (3) to (11) supply all characteristic values of the propeller if the mean value factor κ of the induced tangential velocities is known. Only moderate accuracy is required for determination of this factor, since the induced velocities were assumed to be small. Ordinary propellers in not extraordinary operating conditions differ so little from the propeller with the minimum induced loss of energy [1] that one can use the numerical values for the mean value factor κ of the optimum propeller, known from Goldstein's exact calculation of this propeller [3].

III. 2. Bases for Calculation of the Counterrotating Propeller

The following assumptions are added to the ones valid for the single propeller. The induced vlocities for the propeller with a finite number of blades are distributed in the slipstream periodically over the circumference of the circle with maximum values in the projection of the blade. (See fig. 3.) If two propellers of finite blade number work one closely behind the other, each of them works because of the additional velocity of the other propellor which is periodically variable over the circumference in an oncoming flow variable with time; hence, it is subject to periodically changing air forces and produces therefore additional velocities changing periodically with time. The course shown in figure 3 will then itself be a mean value of the time over which moreover the variation caused by its partner would have to be superimposed. We calculate with these mean values of the time and thus neglect the unsteady effect due to the fluctuations with time of the induced oncoming flow. Söhngen [13] estimated these forces and found them not to be dangerous as was to be hoped since the induced velocities are small compared with the main velocities.

Here and later on index I will always refer to the front propeller, index II to the rear propeller. $\tilde{w}_{aI}$ and $\tilde{w}_{tI}$ in particular are the induced velocities left in the slipstream by the first propeller, $\tilde{w}_{aII}$ and $\tilde{w}_{tII}$ the contributions produced by the second propeller.

The mean values (see equation 2) (which are constant over the circumference) of the quantities $\tilde{w}_t$ and $\tilde{w}_a$, which are variable over the propeller circumference according to figure 3, are named κw_t and $\kappa' w_a$. We introduce the simplification $\kappa = \kappa'$ which is also usual in the theory of the single optimum propeller. These mean values take the course indicated in figure 4 in the direction of the slipstream. Since we assume that the two propeller partners are

arranged one closely behind the other and have equal and opposite angular velocity $\omega_{II} = -\omega_I$, the value $v + \kappa_{II}\frac{w_{aII}}{2}$ replaces v for the first propeller (if the unsteady effect mentioned above is neglected) whereas no additional term from the second propeller is added to $r\omega_I = r\omega$. For the second propeller v is replaced by the value $v + \kappa_I\frac{w_{aI}}{2}$, $r\omega_{II} = -r\omega$ by the value $-r\omega - \kappa_I w_{tI}$.

Therefore the effective velocity components

$$v + \kappa_{II}\frac{w_{aII}}{2} + \frac{w_{aI}}{2},\ r\omega - \frac{w_{tI}}{2}$$

are acting relative to the blade element of the first propeller, the effective velocity components

$$v + \kappa_I\frac{w_{aI}}{2} + \frac{w_{aII}}{2},\quad -r\omega - \kappa_I w_{tI} - \frac{w_{tII}}{2}$$

relative to the blade element of the second propeller. Hence the mean axial velocity far behind the propeller is

$$v + \kappa_I w_{aI} + \kappa_{II} w_{aII}$$

the mean axial velocity at the propeller disk in the propeller plane

$$v + \kappa_I\frac{w_{aI}}{2} + \kappa_{II}\frac{w_{aII}}{2}$$

the mean rotation in the slipstream

$$\kappa_I w_{tI} + \kappa_{II} w_{tII}$$

If the direction of rotation of the two propellers is opposite the induced tangential velocities have opposite signs (fig. 3). If we consider a circle around the propeller axis far behind the propeller, we find the extreme values of the two curves in general not at the same location so that the resultant $\tilde{w}_{tI} + \tilde{w}_{tII}$ does not

disappear everywhere even if the curves have the same shape, though it disappears on the average $\kappa_I w_{tI} + \kappa_{II} w_{tII}$. Energy losses due to rotation can, therefore, not be completely avoided even for counter-rotating propellers because of the finite number of wings (see also [7]).

Under the assumptions discussed here the formulas for the counter-rotating propeller read as follows. The circulations corresponding to (3) are

$$\left.\begin{aligned} \Gamma_I &= 2r\pi\kappa_I w_{tI} \\ \Gamma_{II} &= 2r\pi\kappa_{II} w_{tII} \end{aligned}\right\} \tag{12}$$

The formulas

$$\left.\begin{aligned} c_{sI}' &= 2\kappa_I \overline{w_{tI}}\left(\overline{r\omega} - \frac{\overline{w_{tI}}}{2}\right) \\ c_{sII}' &= -2\kappa_{II}\overline{w_{tII}}\left(\overline{r\omega} + \kappa_I \overline{w_{tI}} + \frac{\overline{w_{tII}}}{2}\right) \end{aligned}\right\} \tag{13}$$

correspond to the formulas (10) for the connection between thrust and induced velocities, the equations

$$\left.\begin{aligned} c_{l_I}' &= 2\overline{r\omega}\kappa_I \overline{w_{tI}}\left(1 + \kappa_{II}\frac{\overline{w_{aII}}}{2} + \frac{\overline{w_{aI}}}{2}\right) \\ c_{l_{II}}' &= -2\overline{r\omega}\kappa_{II}\overline{w_{tII}}\left(1 + \kappa_I\frac{\overline{w_{aI}}}{2} + \frac{\overline{w_{aII}}}{2}\right) \end{aligned}\right\} \tag{14}$$

to the relations (11) for the power loading. We add another relation for the total c_s' of the counterrotating propeller. (Symbols without index I or II will refer to the total arrangement.) From the momentum theory for the propeller with an infinite number of blades

$$c_s' = 2\overline{w_a}\left(1 + \frac{\overline{w_a}}{2}\right)$$

there follows

$$1 + \frac{\overline{w_a}}{2} = \frac{1}{2}\left(1 + \sqrt{1 + c_s'}\right) \tag{15}$$

$1 + \frac{\overline{w_a}}{2}$ is the axial velocity acting at the location of the propeller.

For the counterrotating propeller with an infinite number of blades (15) with the axial velocity at the propeller disk acting at the location of the propeller

$$1 + \frac{\overline{w_{a_I}}}{2} + \frac{\overline{w_{a_{II}}}}{2}$$

is valid. The mean axial velocity at the propeller disk for the counterrotating propeller with a finite number of blades is

$$1 + \kappa_I \frac{\overline{w_{a_I}}}{2} + \kappa_{II} \frac{\overline{w_{a_{II}}}}{2}$$

We shall neglect the square of the variation velocities $\overline{w}_a - \kappa w_a$ and shall use the approximation

$$1 + \kappa_I \frac{\overline{w_{a_I}}}{2} + \kappa_{II} \frac{\overline{w_{a_{II}}}}{2} \approx \frac{1}{2}\left(1 + \sqrt{1 + c_s'}\right) \tag{17}$$

as relation for checking purposes.

In order to be able to proceed to the formulas for the blade element we have to consider first the analogon to figure 2, namely the figure 5. The corresponding figure in Kramer's treatise [7] is valid for the special irrotational condition; the same representation was selected for the rest. One can see the significance of the single lines from the figure title. Since we interpreted the influence of the other propeller upon the one under consideration as variation of

the oncoming flow toward the first propeller, it is clear after what has been said in section III 1. that the velocity induced by the propeller itself $\frac{w_n}{2}$ is perpendicular to the actual oncoming flow which contains simultaneously the influence of the other propeller. These are the right angles specially marked in figure 5 by means of which one derives from figure 5

$$\tan \varphi_{w_I} = \frac{w_{t_I}}{w_{a_I}} = \frac{1 + \kappa_{II}\frac{\overline{w_{a_{II}}}}{2} + \frac{\overline{w_{a_I}}}{2}}{r\bar{\omega} - \frac{\overline{w_{t_I}}}{2}}$$

$$\tan \varphi_{w_{II}} = -\frac{w_{t_{II}}}{w_{a_{II}}} = \frac{1 + \kappa_I\frac{\overline{w_{a_I}}}{2} + \frac{\overline{w_{a_{II}}}}{2}}{\overline{r\omega} + \kappa_I\,\overline{w_{t_I}} + \frac{\overline{w_{t_{II}}}}{2}} \qquad (18)$$

(on the second propeller all angles in the opposite sense are designated as positive). One can see that one now must define instead of the angle of advance two angles

$$\varphi_I^* = \varphi + \alpha_{II}^*$$

$$\varphi_{II}^* = \varphi + \alpha_I^* \qquad (19)$$

α_{II}^* represents the change of direction produced by the second propeller on the first one, α_I^* the change of direction produced by the first on the second one. (α_I^* is negative in fig. 5.) We designate the pertaining ratios of advance as

$$\left.\begin{aligned} \lambda_I^* = x \tan \varphi_I^* &= x \frac{1 + \kappa_{II} \frac{\overline{w_{a_{II}}}}{2}}{\overline{rw}} \\ \lambda_{II}^* = x \tan \varphi_{II}^* &= x \frac{1 + \kappa_I \frac{\overline{w_{a_I}}}{2}}{\overline{rw} + \kappa_I \overline{w_{t_I}}} \end{aligned}\right\} \quad (20)$$

Then the equations (6) assume the shape

$$\left.\begin{aligned} c_{a_I} &= \frac{8x}{z \frac{l}{R}} \kappa_I \sin (\beta_{Id} - \alpha_{Id}) \tan \left[\beta_{Id} - (\varphi + \alpha_{II}^*) - \alpha_{Id}\right] \\ c_{a_{II}} &= \frac{8x}{z \frac{l}{R}} \kappa_{II} \sin (\beta_{IId} - \alpha_{IId}) \tan \left[\beta_{IId} - (\varphi + \alpha_I^*) - \alpha_{IId}\right] \end{aligned}\right\} \quad (21)$$

These equations must be equated to the relations known from the measurements of the polars $c_{aI}(\alpha_{Id})$ and $c_{aII}(\alpha_{IId})$. For the thrust coefficients with friction loss one obtains, corresponding to (8),

$$\left.\begin{aligned} \frac{dk_{s_I}}{dx} &= \frac{z}{\pi} \frac{l}{R} (x^2 + \lambda_I^{*2}) c_{aI} \cos^2 \alpha_{i_I} \cos (\varphi_{wI} + \gamma_I) / \cos \gamma_I \\ \frac{dk_{s_{II}}}{dx} &= \frac{z}{\pi} \frac{l}{R} (x^2 + \lambda_{II}^{*2}) c_{aII} \cos^2 \alpha_{i_{II}} \cos (\varphi_{wII} + \gamma_{II}) / \cos \gamma_{II} \end{aligned}\right\} \quad (22)$$

and for the power coefficients, corresponding to (9),

$$\frac{dk_{zI}}{dx} = \frac{dk_{sI}}{dx} x \tan\left(\varphi_{wI} + \gamma_I\right)$$

$$\frac{dk_{zII}}{dx} = \frac{dk_{sII}}{dx} x \tan\left(\varphi_{wII} + \gamma_{II}\right) \tag{23}$$

One derives from (22) for the local thrust loadings without losses

$$c_s' = \frac{dc_s}{d(x^2)} = \frac{1}{2x}\frac{dc_s}{dx} = \frac{1}{2x}\frac{1}{\lambda^2}\left(\frac{dk_s}{dx}\right)_{\varepsilon_p=0}$$

$$\left.\begin{aligned} c_{sI}' &= \frac{z}{\pi}\frac{l}{R}\frac{1}{\lambda^2}\frac{1}{2x}\left(x^2 + \lambda_I^{*2}\right) c_{aI} \cos^2\alpha_{iI} \cos\varphi_{wI} \\ c_{sII}' &= \frac{z}{\pi}\frac{l}{R}\frac{1}{\lambda^2}\frac{1}{2x}\left(x^2 + \lambda_{II}^{*2}\right) c_{aII} \cos^2\alpha_{iII} \cos\varphi_{wII} \end{aligned}\right\} \tag{24}$$

The formulas correspond to those for the single propeller with the exception of the unknown small additional angles α_I^* and α_{II}^*; their determination by a method of iteration (single iteration) shall be treated below. The equations (13) will be used for determination of the induced velocities; therefore, we write them in the shape

$$\overline{w_{t_I}} = \overline{rw} - \sqrt{\overline{rw}^2 - \frac{c_{sI}'}{\kappa_I}} \tag{25a}$$

$$-\overline{w_{t_{II}}} = \overline{rw} + \kappa_I \overline{w_{t_I}} - \sqrt{\left(\overline{rw} + \kappa_I \overline{w_{t_I}}\right)^2 - \frac{c_{sII}'}{\kappa_{II}}} \tag{25b}$$

The method was tested on a propeller measured by Lesley [9]. Lesley made two ordinary two-blade propellers work as counter-rotating propeller. Hence the blade contour was not changed in any way for the counterrotating propeller and we could hope that the mean value factors κ indicated by Goldstein and Lock (see for instance in [14]) would suffice.

IV. METHOD FOR VERIFICATION OF THE CALCULATION OF THE COUNTER-ROTATING PROPELLER AND COMPARISON WITH MEASUREMENTS

(a) Multisection Method

The calculation is made exactly as in Walchner's method [14]. The initial values are $\alpha_I^* = \alpha_{II}^* = 0$ (no mutual influence). On the sheet Ib and IIb, respectively, the value α_d is determined by trial; c_{aI} or c_{aII} for this value agrees according to (27) with the value from the profile polars $c_{aI}(\alpha_{Id})$ or $c_{aII}(\alpha_{IId})$. The equations (24) give, with c_{aI} and c_{aII}, as a result c_{sI}' and c_{sII}'. (See sheet Ia and IIa, Step 1.) On the right part of sheet Ia, at the top, (Step 1) w_{tI} and w_{tII} are determined from c_{sI}' and c_{sII}' according to (25a) and (25b). Below (Step 1) a first approximation for $\overline{w_{aI}}$ and $\overline{w_{aII}}$ is calculated from the first relation (18)

$$\left.\begin{aligned} \tan \varphi_{w_I} &= \frac{\overline{w_{t_I}}}{\overline{w_{a_I}}} \\ \tan \varphi_{w_{II}} &= -\frac{\overline{w_{t_{II}}}}{\overline{w_{a_{II}}}} \end{aligned}\right\} \qquad (18a)$$

Then the second relation (18)

$$\left.\begin{aligned} \frac{\overline{w_{t_I}}}{\overline{w_{a_I}}} &= \frac{1 + \kappa_{II}\frac{\overline{w_{a_{II}}}}{2} + \frac{\overline{w_{a_I}}}{2}}{\overline{rw} - \frac{\overline{w_{t_I}}}{2}} \\ \frac{\overline{w_{t_{II}}}}{\overline{w_{a_{II}}}} &= \frac{1 + \kappa_I\frac{\overline{w_{a_I}}}{2} + \frac{\overline{w_{a_{II}}}}{2}}{\overline{rw} + \kappa_I\overline{w_{t_I}} + \frac{\overline{w_{t_{II}}}}{2}} \end{aligned}\right\} \qquad (18b)$$

is interpreted as equation for $\overline{w_{a_I}}$ and $\overline{w_{a_{II}}}$: the first approximation is inserted on the right and thus a second approximation obtained. The procedure is repeated for control; usually no more change occurs if one limits oneself to 3 digits (4th digit estimated). (18b) gives more satisfactory results than (18a) for the reason that one must calculate with the value φ_w from the first step (without mutual influence) in (18a), whereas (18b) contains already a better value for φ_w (with mutual influence). λ_I^* and λ_{II}^* are determined with $\overline{w_{a_I}}$ and $\overline{w_{a_{II}}}$ according to (20) and therewith the initial values for the second iteration step obtained.

Whereas one has to take κ (which is a function of $x \tan \varphi_w$ a value unknown at first) for the first step from $\lambda = x \tan \varphi$, the value $x \tan \varphi_w$ for the second step is given by (18b) with sufficient accuracy.

One selects for the calculation for the further sections $x = \text{const.}$ the value at $x \tan \varphi_w$ of the first section (see also [14]) as initial values for κ, because $x \tan \varphi_w$ is constant over the radius for the optimum propeller. The good agreement of this value with the values $x \tan \varphi_w$ obtained by further calculation showed that the use of the κ-values of the optimum propeller for the present case was justified.

The second step (sheet Ia, IIa, Step 2 is performed exactly like the first; the necessity might arise to calculate a third approximation for c_{sI}' and c_{sII}'. It proved always to be unnecessary to do the auxiliary calculation for a third time since λ_I^* and λ_{II}^* did not change any more after the Step 2.

$c_s' = c_{sI}' + c_{sII}'$ was always substituted into the equation for checking

purposes (17). (See sheet Ia, left, below.) Once the ϵ_p-values for the respective Reynolds numbers are obtained one can calculate $\frac{dk_s}{dx}$ and $\frac{dk_l}{dx}$. The method for counterrotating propellers takes somewhat more than four times the time spent on calculations for the method for single propellers.

The calculation of the propeller measured by Lesley was verified for several ratios of advance. The data $\frac{l}{R}$, $\frac{d}{l}$, and β_d of the propeller may be taken from [10]. There was no purpose in looking for statements about the profile or for profile polars as one can hardly assume that these polars would be found just at the Reynolds number of the test. It was therefore assumed that the profiles as propeller blade elements are not very different from the Göttingen series 622-25 and that one may coordinate to each profile the Göttingen profile corresponding to its thickness. The curves $c_a(\alpha_d)$ of the Göttingen series were linearized and pitch and zero lift were plotted over the thickness parameter $\frac{d}{l}$. From these curves, a

$$c_a = \frac{dc_a}{d\alpha} \alpha_d + c_{a0}$$

could be coordinated to each profile measured according to its thickness. The resultant velocity $w = \sqrt{v^2 + (r\omega)^2}$ could be calculated for each section from the statements in [9]; with w the Reynolds number $Re = \frac{wl}{\upsilon}$ could then be formed. From the Göttingen profiles, measured for various small Reynolds numbers (see [15]) one could then coordinate by interpolation according to the thickness parameter to each profile measured its drag-lift coefficient.

Table I shows the results of the verification of the calculation of the counterrotating propeller measured by Lesley which was thus performed. First, one must admit that measurement and calculation do not agree too well; one may give various explanations for this fact. The coordination of the unknown profiles to the Göttingen series certainly constitutes a crude procedure. The determination

of ϵ_p is very uncertain. The calculation of the pertaining single four-blade propeller, also measured by Lesley, was verified for the same ratios of advance by means of the Walchner method [14] for the single propeller in order to decide on the reason for the deviation; the same systematic difference between calculation and measurement was found as in the case of the counterrotating propeller (See table I.) Therefore, the deviations are not caused by the method for the counterrotating propeller but by the coordination of the profiles to the Göttingen series whereby the profile properties are, after all, not correctly covered. The differences in the characteristic numbers between single and counterrotating propellers show an approximate agreement with the measurement.

IV. (b) Single Section Method (Method of Polars).

The iteration method described above which takes the mutual influence of the two propellers into consideration can be applied as well to a single section method (method of polars according to von Doepp in the shape amended by Kramer [8]) as to a multi-section method (Walchner's method [14]). If the polar of the single partner for the respective blade angle is known, one can calculate the counterrotating propeller by application of the method of iteration to the section $\sigma = 0.7$. If one wants to use the same polar for both partners the blade angles must not deviate too much from the blade angle on which the polar is based; this condition is certainly met for the optimum case. Moreover, Kramer's method is based on the circulation of Betz' optimum propeller. For other contours the constants of the method would have to be changed. The example demonstrates best the method of calculation for the counterrotating propeller (see computation sheets IIIa to IV). Since Lesley measured the parts of the counterrotating propeller also as single propeller one was in a position to procure at first according to Kramer's method the polar of the single partner (see computation sheet IIIb) and by means of it to calculate the counterrotating propeller. The advantage as compared with the example calculated by means of the multisection method was that now the profile properties of the measured propeller actually enter into the calculation. The calculation for both partners is made as in Kramer's method for the first step. The calculation course indicated there [8] is used and supplemented by the values

$$c_s = \frac{k_s}{\lambda^2}$$

$$c_{s\sigma}' = \left(\frac{dc_s}{dx^2}\right)_\sigma = 1.273 c_s$$

The auxiliary calculation (computation sheet IIIa, right) is performed with the values c_{sI}' and c_{sII}' exactly as in the multisection method (computation sheet I a). The values

$$\left.\begin{aligned} \lambda_{I\sigma}{}^{*} = \sigma \tan \varphi_{I\sigma}{}^{*} &= \sigma \left(\frac{1 + \kappa_{II} \frac{\overline{w_{a_{II}}}}{2}}{r\omega} \right)_{\sigma} \\ \lambda_{II\sigma}{}^{*} = \sigma \tan \varphi_{II\sigma}{}^{*} &= \sigma \left(\frac{1 + \kappa_{I} \frac{\overline{w_{a_{I}}}}{2}}{\overline{r\omega} + \kappa_{I} \overline{w_{t_{I}}}} \right)_{\sigma} \end{aligned}\right\} \quad (20)$$

are obtained and therewith $\varphi_{I\sigma}{}^{*}$ and $\varphi_{II\sigma}{}^{*}$ as initial values for the second iteration step. One must only bear in mind for the second step that in the columns 1 to 27 φ_{σ} is now replaced by $\varphi_{\sigma I}{}^{*}$ and $\varphi_{\sigma II}{}^{*}$, respectively, and λ by $\lambda_{I}{}^{*}$ and $\lambda_{II}{}^{*}$.

Therefore, in these formulas the values with an asterisk are used; for the first step (without mutual influence) the values with asterisk equal the ones without asterisk. However, in the columns 28 and 31 the original values tan φ_{σ} and λ must be inserted for the iteration also, for they belong to the formula

$$\eta = \frac{\lambda k_{s}}{k_{l}}$$

One can notice on the computation sheets, below at the right, that it was preferred to use the κ-curves instead of working with the curves f_{σ} indicated by Kramer, partly because the κ is needed for the auxiliary calculation, but mainly because more accurate values for f_{σ} could be obtained in this way. The agreement of the calculated with the measured values is satisfactory. (See table I.)

V. PROPERTIES OF THE COUNTERROTATING PROPELLER AND DESIGN REQUIREMENTS

1. For the Case of Maximum Compensation for Rotation

(a) Proportional thrust and power.

The measurements and verifications of calculations will be dealt with again later on after several properties of the counterrotating propeller have been clarified. As mentioned in the introduction the two partners are supposed to agree in all properties excepting the variation of the blade angle. The value of this parameter is left undecided and with it the slipstream for the advance ratio of the design is obtained. The simple equations (13) and (14) are used for the basic investigations, only the relations at the section r are considered and the question of thrust distribution over the radius is left open which does not solely depend upon aerodynamic view points.

The optimum condition is characterized by the fact that the rotation in the slipstream disappears on the average

$$\kappa_I w_{t_I} + \kappa_{II} w_{t_{II}} = 0 \tag{26}$$

The induced angle of advance of the two propellers then shows so little difference that the difference can be hardly determined for the κ-values. Therefore one may presume

$$\kappa_I = \kappa_{II} = \kappa \tag{27}$$

for the irrotational condition; (26) can then be given also in the shape of

$$w_{t_I} + w_{t_{II}} = 0 \tag{26a}$$

(See also [7].) Under these assumptions the equations (13) are written

$$c_{s_I}' = \kappa w_{tI}\left(2\bar{r}\bar{\omega} - \overline{w_{tI}}\right)$$

$$c_{sII}' = \kappa \overline{w_{tI}}\left(2\bar{r}\bar{\omega} + 2\kappa\overline{w_{tI}} - \overline{w_{tI}}\right) \qquad (13a)$$

There follows for the total c_s'

$$c_s' = 2\left[2\kappa \overline{w_{tI}}\bar{r}\bar{\omega} - \kappa\overline{w_{tI}}^2(1 - \kappa)\right] \qquad (28)$$

The first equation (13a) represents the local thrust loading of a single propeller which corresponds in all data to a partner of the counterrotating propeller. One can see from the equation (28) that the counterrotating propeller not only produces twice the thrust but that the second propeller recovers additionally the contribution $2\kappa^2\overline{w_{tI}}^2$ from the slipstream. One can further see that the recovery of rotation increases with increasing number of blades (increasing κ) and that it is better in the proximity of the hub (larger κ-values and larger $\overline{w_t}$-values) than outside.

Taking the fact into consideration that the term $(1 - \kappa)\kappa\overline{w_{tI}}^2$ in (28) is small the distribution of thrust on the two partners can be written

$$c_{sI}' = \frac{c_s'}{2} - \kappa^2\overline{w_{tI}}^2 \approx \frac{c_s'}{2} - \left(\frac{c_s'}{4\bar{r}\bar{\omega}}\right)^2$$

$$c_{sII}' = \frac{c_s'}{2} + \kappa^2\overline{w_{tI}}^2 \approx \frac{c_s'}{2} + \left(\frac{c_s'}{4\bar{r}\bar{\omega}}\right)^2 \qquad (29)$$

or

$$\left.\begin{aligned} k_{sI}' &\approx \frac{k_s'}{2} - \left(\frac{k_s'}{4x}\right)^2 \\ k_{sII}' &\approx \frac{k_s'}{2} + \left(\frac{k_s'}{4x}\right)^2 \end{aligned}\right\} \qquad (30)$$

For the condition of the slipstream which is irrotational on the average $\kappa(w_{tI} + w_{tII}) = 0$ (see equations (26) and (27) there follows from (14) for the local power loadings

$$\left.\begin{aligned} c_{zI}' &= 2\bar{r}\bar{\omega}\kappa\overline{w_{tI}}\left(1 + \kappa\frac{\overline{w_{aII}}}{2} + \frac{\overline{w_{aI}}}{2}\right) \\ c_{zII}' &= 2\bar{r}\bar{\omega}\kappa\overline{w_{tI}}\left(1 + \kappa\frac{\overline{w_{aI}}}{2} + \frac{\overline{w_{aII}}}{2}\right) \end{aligned}\right\} \qquad (31)$$

Since the thrusts according to (29) do not differ widely for the irrotational condition, the first order expressions of the axial velocities w_{aI} and w_{aII} also do not differ (see equation (18b); moreover they were presupposed (small load) to be small compared with 1 so that the terms in parenthesis in (31) are practically identical. The irrotational condition therefore equals the condition of equal power absorption of the two partners. Therewith the moment equilibrium for the same number of revolutions also is given. From the sum of the equations (31) follows that the power absorption is by the small amount $2\bar{r}\bar{\omega}\kappa^2\overline{w_t}\overline{w_a}$ superior to the double power of a single partner.

(b) Gain in efficiency and increased power absorption

It was mentioned already that the terms in parentheses in (31) can be equated; for abbreviation, the velocity v_1 is introduced

$$\overline{v_1} = 1 + \kappa\frac{\overline{w_{aI}}}{2} + \frac{\overline{w_{aII}}}{2} \approx 1 + \kappa\frac{\overline{w_{aII}}}{2} + \frac{\overline{w_{aI}}}{2} \qquad (32)$$

Then

$$\eta_{igz} = \frac{c_s}{c_l} = \frac{2\kappa\overline{r\omega w_t} - \kappa(1-\kappa)\overline{w_t^2}}{2\kappa\overline{r\omega w_t}\overline{v_1}} = \frac{1}{\overline{v_1}}\left[1 - \frac{\overline{w_t}}{2\overline{r\omega}}(1-\kappa)\right] \qquad (33)$$

is valid for the irrotational condition. η_{igz} stands for the ideal efficiency of a counterrotating propeller each partner of which has the number of blades z so that the counterrotating propeller has the blade number $2z$. The formula shows what can be gained by an increase of the number of blades: for $z = \infty$ ($\kappa = 1$) there results the maximum theoretical efficiency

$$\eta_a = \frac{1}{\overline{v_1}} = \frac{1}{1 + \frac{\overline{w_{aI}}}{2} + \frac{\overline{w_{aII}}}{2}} \approx \frac{1}{1 + \overline{w_a}} \qquad (34)$$

The local efficiency of the counterrotating propeller of the blade number $2z$ is now compared with the local efficiency of a single propeller of the blade number z. The two propellers shall agree in the local ratio of advance $\frac{v}{r\omega}$. The single propeller which produces the same $\overline{w_t}$ and, because of $\frac{w_t}{w_a} \approx \frac{v}{r\omega}$ (see fig. 2 or 5) also the same $\overline{w_a}$ as a partner of the counterrotating propeller is first considered for comparison; then the counterrotating propeller is compared with the single propeller which produces twice the $\overline{w_t}$ and therefore also twice the $\overline{w_a}$ as a partner of the counterrotating propeller. Considering the connection (10) or (11) of the induced velocities with the thrust loading and the power loading the first of the compared propellers is to a first order approximation the one with

half the power of the counterrotating propeller, the second the one with the same power as the counterrotating propeller. The second case is treated first because it is more interesing in practice; therefore the efficiency of equation (33) is compared with the efficiency of the single propeller of the induced velocities $2\overline{w_t}$ and $2\overline{w_a}$ according to equations (10) and (11)

$$\eta_{iezk_1} = \frac{4\kappa\overline{rw}\,\overline{w_t} - 4\kappa\overline{w_t}^2}{4\kappa\overline{rw}\,\overline{w_t}(1 + \overline{w_a})} = \frac{1}{1 + \overline{w_a}}\left(1 - \frac{\overline{w_t}}{\overline{rw}}\right)$$

$$= \frac{1}{v_1}\left[1 - \frac{w_t}{rw} - (1 - \kappa)\frac{w_a}{2v_1}\right]$$

Then there results with (33)

$$\eta_{igz} - \eta_{iezk_1} = \frac{1 + \kappa}{2}(\eta_a - \eta_{iezk_1}) + \frac{(1 - \kappa)w_a}{2v_1} \qquad (35a)$$

The last term is in any case $< \frac{w_a}{2}$. For large values of λ, for which the counterrotating propeller is particularly effective, $w_a << w_t$. The difference in efficiency which has to be determined becomes at least

$$\eta_{igz} - \eta_{iezk_1} \gtrsim \frac{1 + \kappa}{2}(\eta_a - \eta_{iezk_1}) \qquad (35b)$$

The axial efficiency is known if one knows ratio of advance and power coefficient, for from the momentum theory (15) there follows immediately (see also [4], p. 182)

$$\frac{1 - \eta_a}{\eta_a^3} = \frac{k_1}{4}\frac{1}{\lambda^3} \tag{36}$$

The formulas (35) indicate that at least the fraction $\frac{1 + \kappa}{2}$ of the loss in rotation (between η_a and η_{ie}) represented in figure 1 can be recovered. (See fig.1.) For an infinite number of blades $\kappa = 1$ the loss in rotation disappears and η_{ig} becomes $\eta_{ig} = \eta_a$.

Then the efficiency of the counterrotating propeller is compared with the efficiency of two independent single propellers of the same number of blades z which each produce the same w_t and w_a as one partner of the counterrotating propeller which therefore to a first order approximation together absorb the same power as the counterrotating propeller (or each one-half of that power). Their ideal local efficiency then is

$$\eta_{iez}\frac{k_1}{2} = \frac{2\kappa r\omega\bar{w}_t - \kappa\bar{w}_t^2}{2\kappa r\omega\bar{w}_t\left(1 + \frac{\bar{w}_a}{2}\right)} = \frac{1}{1 + \frac{\bar{w}_a}{2}}\left(1 - \frac{w_t}{2r\omega}\right)$$

$$= \frac{1}{v_1}\left(1 - \frac{w_t}{2r\omega} + \kappa\frac{w_a}{2v_1}\right)$$

If one compares it with the efficiency of the counter-rotating propeller (33), one obtains

$$\eta_{igz} - \eta_{iez}\frac{k_1}{2} = \kappa\left(\eta_a - \eta_{iez}\frac{k_1}{2}\right) \tag{37}$$

It has been seen above that the counterrotating propeller is slightly superior to both the separately moving propellers with respect to both

thrust and power. It is therefore questionable whether and under what conditions it is superior to them with respect to efficiency, when therefore the difference indicated in equation (37) is positive. The efficiency of the counterrotating propeller and the maximum theoretical efficiency appearing on the right side of (37) refer to a propeller which absorbs twice the power of the single propeller considered for comparison. Therefore it would have to be inferior in efficiency to the propeller used for comparison, if the rotational losses of the compared propeller are not so large as to neutralize the deterioration of efficiency due to the double power required just by avoiding these losses (η_a does not contain losses in rotation, η_{igz} only residual losses due to rotation). Therefore one will ask oneself for what operating conditions the axial efficiency η_a of the propeller of double power will be higher than the ideal efficiency of the single propeller, when therefore

$$\frac{1}{1 + \overline{w_a}} > \frac{1}{1 + \frac{\overline{w_a}}{2}}\left(1 - \frac{\overline{w_t}}{2r\omega}\right)$$

is valid. If one sets again

$$\frac{w_t}{w_a} \approx \frac{v}{r\omega}$$

the result of the calculation will be

$$\frac{v}{r\omega} = \frac{\lambda}{x} > 1 \qquad (38)$$

This relation is supported by measurements [9] and can also be found in Pistolesi [11]. The formulas (35) and (37) show satisfactory agreement with Kramer's statements [7]. To evaluate them one takes the axial efficiency from (36), the ideal efficiency of the single propeller for instance from [6].

In immediate conjunction there arises the question by what amount the power absorption of a counterrotating propeller (number of blades 2z) can be increased as compared to a single propeller (number of blades z) for large ratios of advance, without making the efficiency drop below the efficiency of this single propeller. The first order expressions of absorbed powers are, according to (11) or (31) proportional to the induced velocities. If one designates for the following calculation the induced velocities of the counterrotating propeller by the index 1, the induced velocities of the single propeller by the index 2,

$$\eta_{igz} = \eta_{iez}$$

will be valid, or, taking the equation (32) into consideration which can also be written $w_{aI} = w_{aII} = w_a$ according to (33) and page 26

$$\frac{1}{1 + \frac{1 + \kappa}{2}\bar{w}_{a1}}\left[1 - \frac{w_{t1}}{2r\omega}(1 - \kappa)\right] = \frac{1}{1 + \frac{\bar{w}_{a2}}{2}}\left(1 - \frac{w_{t2}}{2r\omega}\right)$$

$$\frac{1 + \kappa}{2}\bar{w}_{a1} + \frac{1 - \kappa}{2\overline{r\omega}}\overline{w_{t1}} = \frac{\overline{w_{a2}}}{2} + \frac{\overline{w_{t2}}}{2\overline{r\omega}}$$

The first order expression of $\overline{w_a}$ is always $\overline{w_a} = \overline{w_t}\frac{\overline{r\omega}}{v} = \overline{w_t}\overline{r\omega}$.

If this expression is inserted, the last equation will read

$$\frac{w_{t1}}{w_{t2}} = \frac{\overline{r\omega} + \frac{1}{\overline{r\omega}}}{(1 + \kappa)\overline{r\omega} + \frac{1 - \kappa}{\overline{r\omega}}}$$

or

$$\frac{w_{t1}}{w_{t2}} = \frac{1 + \left(\frac{\lambda}{x}\right)^2}{(1 + \kappa) + (1 - \kappa)\left(\frac{\lambda}{x}\right)^2}$$

The proportionality of the induced velocities and the power loading mentioned above reads, according to (31) and (11),

$$c_{l_g} = 4\overline{r_0}\kappa\overline{w_{t1}}\left(1 + \frac{1 + \kappa}{2}\overline{w_{a1}}\right) \approx 4\overline{r_0}\kappa\overline{w_{t1}}$$

$$c_{l_e} = 2\overline{r_0}\kappa\overline{w_{t2}}\left(1 + \frac{\overline{w_{a2}}}{2}\right) \approx 2\overline{r_0}\kappa\overline{w_{t2}}$$

Hence follows

$$\frac{c_{l_g}}{c_{l_e}} = \frac{2w_{t1}}{w_{t2}} = 2\frac{x^2 + \lambda^2}{(1 + \kappa)x^2 + (1 - \kappa)\lambda^2} = \frac{1 + \left(\frac{\lambda}{x}\right)^2}{\frac{1 + \kappa}{2} + \frac{1 - \kappa}{2}\left(\frac{\lambda}{x}\right)^2} \qquad (39)$$

For the local ratio of advance $\frac{\lambda}{x} = 1$ one obtains the result that for the same ideal efficiency the power absorption of the counterrotating propeller with the number of blades $2z$ equals exactly double the power absorption of the single propeller with the blade number z as one knew already from equation (38). The superiority of the counterrotating propeller over the single propeller for large ratios of advance is also shown in equation (39) since the proportional power absorption for the same ideal efficiency increases with the ratio of advance. For complete recovery of rotation ($\kappa = 1$) there even results an increase with the second power of λ of this proportional

power absorption. However, a counterrotating propeller of finite number of blades leaves behind residues of rotation in the slipstream which increase with the ratio of advance because of the decrease of κ with λ (see for instance [14]). The equation (39) yields for each number of blades $2z$ of the counterrotating propeller an optimum λ for which the increase in power reaches a maximum as compared with the single propeller of the number of blades z. The limiting value for $\frac{c_{lg}}{c_{le}}$ for an infinite ratio of advance $\frac{\lambda}{x}$ has according to (39) a value of 2.

The limiting value η_{igz} of the counterrotating propeller with a finite number of blades tends because of the unavoidable residual losses due to rotation exactly like the limiting value η_{iez} of the single propeller for $\lambda \longrightarrow \infty$ toward zero (See fig. 1.)

V. 1. (c) Variation of the blade angle

The desirable irrotational condition can be obtained by a suitable difference of the blade angle which is dependent on r. Irrotationality $\kappa_I w_{tI} + \kappa_{II} w_{tII} = 0$ means equality of circulation. If one assumes the blade angle referred to the direction of the zero lift of the profile, one can write, according to (4)

$$\Gamma = \frac{l}{2} \frac{dc_a}{d\alpha} w_w(\beta - \varphi_w)$$

Since the difference of the two blade angles $\beta_I - \beta_{II}$ will be calculated, the term of the reference direction is again eliminated for the same profiles in the same section so that one can understand again by β the blade angle referred to the pressure side. Therefore,

$$w_{wI}(\beta_I - \varphi_{wI}) = w_{wII}(\beta_{II} - \varphi_{wII}) \qquad (40)$$

is valid. If one substitutes at first the values for the effective velocities of oncoming flow for the irrotational condition, one obtains

$$\sqrt{v_1^2 + \left(r\omega - \frac{w_t}{2}^2\right)(\beta_I - \varphi_{wI})} = \sqrt{v_1^2 + \left(r\omega + \kappa_I w_t - \frac{w_t}{2}^2\right)(\beta_{II} - \varphi_{wII})}$$

or neglecting higher order terms,

$$\beta_I - \varphi_{wI} = \left[1 + \frac{r\omega\kappa w_t}{v_1^2 + (r\omega)^2}\right](\beta_{II} - \varphi_{wII}) \tag{41}$$

For the small angle $\varphi_{wI} - \varphi_{wII}$ one can substitute its tangent which can be calculated according to (18). The angle $\varphi_{wI} - \varphi_{wII}$ is

$$\varphi_{wI} - \varphi_{wII} \approx \tan(\varphi_{wI} - \varphi_{wII}) = \frac{\tan\varphi_{wI} - \tan\varphi_{wII}}{1 + \tan\varphi_{wI}\tan\varphi_{wII}}$$

$$= \frac{v_1 \kappa w_t}{v_1^2 + (r\omega)^2}$$

Then one can use $\frac{v_1}{v} = \frac{1}{\eta_a}$ and write for (41)

$$\beta_I - \varphi_{wI} = \beta_{II} - \varphi_{wII} + (\beta_{II} - \varphi_{wII})(\varphi_{wI} - \varphi_{wII})\frac{x\eta_a}{\lambda} \tag{43}$$

Since the angles $\varphi_{wI} - \varphi_{wII}$ and $\beta_{II} - \varphi_{wII}$ are small, the second term on the right is small compared with the first one. It could be of importance only for very small ratios of advance. For high speed conditions, however, there is certainly

$$\beta_I - \beta_{II} = \varphi_{wI} - \varphi_{wII}$$

valid with sufficient accuracy or, according to (42),

$$\beta_I - \beta_{II} = \kappa \frac{w_t}{r\omega} \frac{\frac{v_1}{r\omega}}{1 + \left(\frac{v_1}{r\omega}\right)^2}$$

In addition, the appearing velocities will be expressed by characteristic values of the propeller. From (28) follows

$$c_s' = 4\kappa \frac{w_t}{r\omega}\left(\frac{r\omega}{v}\right)^2$$

therefore

$$\kappa \frac{w_t}{r\omega} = \frac{c_s'}{4}\left(\frac{\lambda}{x}\right)^2$$

and therewith

$$\beta_I - \beta_{II} = \frac{c_s'}{4} \frac{\lambda^3 \eta_a}{x\left[(x\eta_a)^2 + \lambda^2\right]} \qquad (44a)$$

Since the axial efficiency η_a is connected with the power coefficient k_l through (36) one prefers to introduce k_l' instead of c_s', that is, one expresses c_s' by k_l' and η_{ig}

$$\frac{c_g\lambda^3}{k_l} = \eta_{ig}$$

and obtains

$$\beta_I - \beta_{II} = \frac{k_l'}{4} \frac{\eta_{ig}\eta_a}{x\left[\lambda^2 + (x\eta_a)^2\right]}$$

The ideal efficiency η_{ig} of the counterrotating propeller could be procured according to (35) or (37) from the ideal efficiency of the corresponding single propeller (with the whole or half the power). However, from (35) and (37) follows that η_{ig} does not much differ from η_a for the irrotational condition. Certainly the dependency on the load (k_l), on the ratio of advance λ and on the radius x is more important for the difference in the pitching angles than the slight difference between η_{ig} and η_a; one may therefore use

$$\beta_I - \beta_{II} = \frac{k_l'}{4} \frac{\eta_a^2}{x\left[\lambda^2 + (x\eta_a)^2\right]} \qquad (44b)$$

as serviceable approximation: all the values are now known directly since η_a is known immediately through (36) from k_l' and λ.

The blade-angle difference increases with increasing and with decreasing x. The dependence on the ratio of advance is rather complicated. The formula (44) is not admissible for very small λ's. For medium λ's the dependence of the formulas (44) on λ is not very extensive because of the increasing of η_a with λ for a fixed k_l (variable pitch propeller) as well as for a k_l decreasing with λ. This fact was demonstrated also in verifying computation. The three operating conditions $\lambda = 0.3$, $0.9/\pi$ and 0.2 are calculated with the same $\beta_I - \beta_{II}$ and are approximately equivalent with respect to proportionate power and residual rotation. For larger λ's (for

instance $\lambda > 0$?) η_a does not change much more (See equation 36.) Then the dependence of the blade angle difference on λ is well noticeable until for large λ's the dependence becomes unimportant and the blade angle difference itself very small. The number of blades enters into (44) only through the power coefficient.

The last term in (43) must not be neglected for small λ's; one uses

$$c_{aII} = \frac{dc_a}{d\alpha}(\beta_{II} - \varphi_{wII})$$

and obtains

$$\beta_I - \beta_{II} = \frac{k_l'}{4} \frac{\eta_a^2}{x\left[\lambda^2 + (x\eta_a)^2\right]}\left(1 + \frac{c_{aII}}{\frac{dc_a}{d\alpha}} \frac{x\eta_a}{\lambda}\right)$$

Therefore a larger blade angle difference has to be selected than resulted according to (44).

The blade-angle differences measured by Lesley [9] decrease with decreasing λ, because k_l decreases rapidly with decreasing λ. However, one can control the relation (44) on hand of his measurements. Lesley aspired to having his counterrotating propeller run for the ratio of advance of the highest efficiency with equal power absorption of the two partners. Of course he did not change anything in the variation of the blade angle; on the contrary, he altered the total pitch of the second as compared with the first propeller until he could experimentally determine equal power absorption for both partners. In the actual test on the counterrotating arrangement he specifies only the total values over both propellers. The verification of the calculation with the $\beta_I - \beta_{II}$ given by him showed that the power absorption of the second partner is smaller than the one of the first partner, particularly so for the larger x's. (See table II.) Even the thrust coefficient of the second partner is smaller than the thrust coefficient of the first partner for some cases although the efficiency of the second partner is superior. If one inserts the $\beta_I - \beta_{II}$ of [9] into (44) one has to go to $x = 0.45$

to satisfy the formula, and there the verification of the calculation had showed also equality in power. (See table II.) If one substitutes $x = 0.7$ into (44) a smaller $\beta_I - \beta_{II}$ is obtained. If one checks the calculation of the propeller using this value the condition of power equality and absence of rotation is actually much better satisfied, particularly for the $x>0.6$. (See table II.)

Since in each propeller the outer blade sections are especially heavily loaded, on the other hand the recovery of rotation is particularly effective in the inner-blade sections one will come to the conclusion that a total adjustment of the second with respect to the first propeller is not satisfactory for the design; one will therefore make the blade-angle difference dependent upon the radius according to (44) (dependence on x and on k_l' (x)). A variable pitch propeller then controls the change to another total pitch distribution exactly as in the case of the single propeller. It ought to be considered whether one could take the dependence of the blade angle difference on the ratio of advance into account. The verification of the calculation of the propeller measured by Lesley proves how unfavorable the blade-angle difference is which is constant over the radius. Although there is equality of power for $x = 0.45$, the contribution of power k_{lII} is no longer more than a third of k_{lI} already for $x = 0.3$. This circumstance is not essential for the propeller which was measured, with its rapid decrease in thrust towards the hub; but it would immediately become important if one would load the hub region according to the optimum more heavily than was done so far.

Summarizing, one can therefore make the following statements concerning the design: The optimum distribution is the distribution of circulation constant over the radius which, however, can not be realized. It must be left to the constructor to find a compromise. The recovery of rotation is larger in the inner-blade regions than in the outer ones. For a selected contour the variation of the blade angle was so far often (see [5])determined from the stipulation that the thrust should disappear simultaneously over the whole blade (aerodynamically not twisted propeller). One will forego the exact fulfillment of this condition for both propellers and will determine the variation of the blade angle difference according to (44). Since $\beta_I - \beta_{II}$ is a small value (a hub radius is cut out) the aerodynamic twist is still small. The total pitch is then determined from the power to be absorbed.

Finally it should be mentioned that estimates concerning section V, 1 may be found in the hitherto existing literature ([11] and [16]).

However, the mutual influence of the two partners is neglected to such an extent that the differences in thrust expressed by (30) and the blade angle difference (44) as being too small are not evident.

V. 2. The Efficiency for Operating Conditions Which Do Not Deviate Much from the Optimum Condition

It shall now be considered how the efficiency is influenced if the counterrotating propeller works in an operating condition which is still so near the condition of equal proportioning of power that (32) can be applied. Then there results from (13) and (14)

$$\eta_{ig} = \frac{c_s}{c_l} = \frac{1}{v_1}\left[1 + \frac{2(1-\kappa)\,\overline{w_{tI}w_{tII}}}{2r\omega\left(\overline{w_{tI}} - \overline{w_{tII}}\right)} - \frac{\left(\overline{w_{tI}} + \overline{w_{tII}}\right)^2}{2r\omega\left(\overline{w_{tI}} - \overline{w_{tII}}\right)}\right] \tag{45}$$

A comparison of this expression with the efficiency for the irrotational condition (33) shows that the two first terms correspond exactly to the terms appearing there since the second term (45) turns into the second term (33) for $w_{tI} = -w_{tII}$. If the w_t-values are small as presupposed, there will be hardly any difference between them. The third term of (45) constitutes the real difference in relation to (33); it contains in the numerator the square of the residual rotation $w_{tI} + w_{tII}$. Therefore the deterioration in efficiency for an operating condition deviating from the condition of maximum compensation of rotation depends upon the residual rotation as was to be expected.

VI. THE BEHAVIOR OF THE PROPELLER OF AN INFINITE NUMBER OF BLADES FROM THE BRAKING DOMAIN UP TO HEAVIER LOADS

1. Development of the Charts

Many problems concerning the operating conditions of the counterrotating propeller for operating conditions which deviate from the condition for the design (condition of minimum loss of rotation) remain still unsolved. In order to obtain a preliminary clue to the behavior of the counterrotating propeller even for extreme cases (if for instance the rear partner works as a windmill) one calculated

and plotted the local thrust loadings of the single propellers for the propeller of an infinite number of blades over a whole region of ratios of advance, form parameters and blade angles; then one arranged the material of curves thus formed in such a manner that one can interpolate.

The equations for the propeller of an infinite number of blades can be written in such a manner that one can solve for a few parameters. The equations (13) with $\kappa = 1$ form the basis of the calculation

$$c_{sI}' = 2\overline{w_{tI}}\left(\overline{r\omega} - \frac{\overline{w_{tI}}}{2}\right) \tag{13$_I$}$$

$$c_{sII}' = -2\overline{w_{tII}}\left(\overline{r\omega} + \overline{w_{tI}} + \frac{\overline{w_{tII}}}{2}\right) \tag{13$_{II}$}$$

Since the induced velocities for the propeller of an infinite number of blades are constant over the circumference of the propeller there remains only the one axial velocity

$$\overline{v_1} = 1 + \frac{\overline{w_{aI}}}{2} + \frac{\overline{w_{aII}}}{2}$$

its partial contributions do not appear any more, and the total c_s' is connected with $\overline{v_1}$ through (17). One selects an expression slightly deviating from (24) for the formulas at the blade. Taking the relation according to definition of c_a (see equation 4) as a basis, one obtains

$$c_{sI}' = \left(\overline{r\omega} - \frac{\overline{w_{tI}}}{2}\right)\sqrt{\overline{v_1}^2 + \left(\overline{r\omega} - \frac{\overline{w_{tI}}}{2}\right)^2}\left(\beta_I - \arctan\frac{\overline{v_1}}{\overline{r\omega} - \frac{\overline{w_{tI}}}{2}}\right)\frac{dc_a}{d\alpha}\frac{l}{2\pi r}z \tag{46$_I$}$$

$$c_{sII}' = \left(\bar{r\omega} + \bar{w}_{tI} + \frac{\bar{w}_{tII}}{2}\right)\sqrt{\bar{v}_1^2 + \left(\bar{r\omega} + \bar{w}_{tI} + \frac{\bar{w}_{tII}}{2}\right)^2}$$

$$\left(\beta_{II} - \arctan \frac{\bar{v}_1}{\bar{r\omega} + \bar{w}_{tI} + \frac{\bar{w}_{tII}}{2}}\right)\frac{dc_a}{d\alpha}\frac{l}{2\pi r}z \qquad (46_{II})$$

All angles here are referred to the direction of zero lift so that one can substitute for c_a

$$c_a = \frac{dc_a}{d\alpha}(\beta - \varphi w)$$

One unites shape and number of the blades into the form parameter

$$A = \frac{dc_a}{d\alpha}\frac{l}{2\pi r}z \qquad (47)$$

One now assumes A and $\bar{r\omega}$ as fixed and investigates the influence of the blade angles β_I and β_{II} upon the two thrust elements. To this end a total c_s' is assumed as given and $\bar{v}_1$ is calculated from (17). For an additionally given β_I, the equations (13_I) and (46_I), when equated, will contain only one unknown value, namely $\bar{w}_{tI}$, and can be solved very quickly for $\bar{w}_{tI}$ by iteration. Simultaneously c_{sI}' and, since c_g' is known, also c_{sII}' are obtained. (13_{II}) can then be solved for $\bar{w}_{tII}$ and (46_{II}) for β_{II} since all other values are known and the unknown appears the first time in the second power, the second time in the first power in the respective equation. Thus one obtains for fixed $\bar{r\omega}$ and A by changing $\bar{c}_s'$ and β_I groups of curves, for instance c_{sI}' and c_{sII}' over β_{II} with β_I as parameter. By changing $\bar{r\omega}$ and A one obtains series of such groups of curves.

VI. 2. Discussion of the Charts

The figures 6 to 8 show several examples. The curves lie approximately linearily between $-1 \leq c_s' \leq 1$. The values c_{sI}' over β_{II} with β_I as parameter are parallel for small values of A and $\bar{r\omega}$, that is, c_{sI}' for small values of A and $\bar{r\omega}$ does not depend on β_{II}. This phenomenon has been known for a long time from tests (see [12]). For larger values of $\bar{r\omega}$ the values of c_{sI}' diminish with increasing β_{II}, that is, with increasing c_{sII}', that is, the increasing load of the second propeller takes effect as reduction of the angle of attack of the first propeller by increase of the angle of advance φ_I^* (equation (20) or fig. 5). However, equation (20) for φ_{II}^* and the figures 6 to 8 also demonstrate that the influence of the first propeller does not always affect the second propeller in same sense. The influence of the first propeller may reduce the angle of attack by increase of φ_{II}^* (c_{sII}' diminishes with increasing β_I as well as increase it (c_{sII}' increases with increasing β_I) by reduction of φ_{II}^* (this case is represented in fig. 5) according to whether the influence of w_{tI} or w_{aI} predominates. w_{tI} prevails for large values of λ and causes the increase of the angle of attack of the second propeller. The superiority of the counterrotating propeller as compared with the single propeller for high values of λ was stressed more than once. (See equations (38) and (39).)

The mutual influence of the two propellers does not depend on the angle of attack only but because of

$$\Gamma = \frac{l}{2} \frac{dc_a}{d\alpha} w_w(\beta - \varphi_w)$$

also on the effect of the then other partner upon the effective oncoming flow. The equations for c_s look somewhat more complicated than the relation for Γ, they contain $v_1 r\omega$ and the induced velocities w_{aI}, w_{tI}, w_{aII}, w_{tII}. If one assumes the relation for c_{sII}' once written with a pair of values w_{aI}', w_{tI}', another time

with another pair of values w_{aII}'', w_{tII}'', one can equate these two relations for c_{sII}' and solve for w_{aII}, w_{tII}. One can coordinate a blade angle to each pair of induced velocities which means that there is a β_{II} to each pair of values β_I' and β_I'' thus, that the same c_{sII}' results for the two values of β_I for this β_{II}. In other words, every two curves c_{sII}' intersect over β_{II} with β_I as parameter as shown in figures 6 to 8. The points of intersection of the curves lie close to each other because the influence of the first upon the second propeller is shown mainly in the variation of the angle of advance. The changing of the angle of advance φ into the angle φ_{II}^* is still more decisive than the influencing of the real angle of advance φ_w. If there were only this main influence effective the same point of intersection would be obtained for all curves, for from

$$\varphi = \varphi_{II}^*$$

follows, as can be easily derived from equation (20) or figure 5,

$$\left(\frac{\lambda}{x}\right)^2 = \frac{1}{2}$$

The region of intersection for small values of $\overline{rw}$ is so located that most of the curves are in the domain where an increase of β_I (that is, of c_{sI}) for constant β_{II} means an increase of c_{sII}'. Just the opposite is true for the large values of $\overline{rw}$. Of course, the relations depend also on the form parameter.

If one examines the verification of the measurement (computation sheet IIa) from this point of view, one will see that the angles φ_{II}^* are larger than φ throughout; the first propeller affects the second by reducing its angle of attack; the appropriate values can be found on the charts c_{sII}' over β_{II} to the left of the region of intersection of the curves. Among the measurements [9] there is only one example ($\lambda = 0.573$), where the verification of the calculation resulted in $\varphi_{II}^* < \varphi$ (See computation sheet IV.)

One now calculated the relations around the region of intersection of the curves c_{sII}' over β_{II} toward both sides over a rather large c_{sII}'-region between about $-0.5 < c_{sII}' < 1$, therefore till into the braking domain. c_{sI}' lies at around 0 to 1. c_{sI}' and c_{sII}' depend in these regions somewhat linearly on β_I as well as on β_{II}. They can therefore be represented as

$$\left.\begin{aligned} c_{sI}' &= (a_1\beta_{II} + b_1)\beta_I + c_1\beta_{II} + d_1 \\ &= a_1\beta_I\beta_{II} + b_1\beta_I + c_1\beta_{II} + d_1 \\ c_{sII}' &= (a_2\beta_I + b_2)\beta_{II} + c_2\beta_I + d_2 \\ &= a_2\beta_I\beta_{II} + b_2\beta_{II} + c_2\beta_I + d_2 \end{aligned}\right\} \quad (48)$$

The coefficients are plotted over $\frac{r\omega}{v}$ with the parameter A (equation(47)) in two charts (figs. 9 and 10). They represent the calculated values not exactly; the deviations for medium c_s'-values amount to about 5%, for very small c_s'-values sometimes to even more. However, they will certainly be smaller than the neglected effects of the finite number of blades and the friction. The charts are supposed to give only a survey over the mutual influence of the two propellers to be expected for various operating conditions. For the rest, the inaccuracy is mainly due to the constants d_1 and d_2. However, the constant is unessential since one will mostly want to take from the charts only the change of the values c_{sI}' and c_{sII}' which occurs when the operating condition is changed.

The coefficients a_1 are smaller than the coefficients a_2, whereas b_1, c_1, and d_1 have the same order of magnitude as the values b_2, c_2, and d_2, as shown by the often stressed fact that the mutual influence is expressed particularly in the effect of the

first propeller upon the angle of attack of the second propeller (main carrier coefficient a_2). The mutual influence divided by the value of the free-stream velocity (mainly expressed in the coefficients c_1 and c_2) is smaller and about equivalent. Actually the connection is very complicated as the curves demonstrate.

VII. SUMMARY

An arrangement for counterrotation is examined; the two partners are arranged close behind one another, have the same diameter, the same shape of blades, equal and opposite angular velocity but deviating course of the blade angles over the radius. For verification of the calculation of the arrangement, the mutual influence of the two propellers can be used in Walchner's method for calculation of the characteristic values of the propeller at the section or into Kramer's single-section method by an iteration method. The difference of the blade-angle course over both partners which is necessary for an optimum utilization of rotation is stated for the design in an easily manageable formula of approximation. Simple formulas are given also for the gain in ideal efficiency to be reached by counterrotation. The investigation shows clearly the operating conditions for which the counterrotation is particularly effective. By efficiency one always understands the local efficiency. The integration over the radius is not carried out because the distribution of circulation over the radius is not solely determined by aerodynamic points of view. The behavior of the counterrotating propeller for various operating conditions from the braking domain up to heavier loads is studied on the propeller with an infinite number of blades. The discussion of the propeller measured by Lesley the calculation of which was verified on a few examples presents an opportunity to examine the results of the treatise.

Translated by Mary L. Mahler
National Advisory Committee
for Aeronautics

VIII. REFERENCES

1. Prandtl, L. and Betz, A.: Vier Abhandlungen zur Hydrodynamik und Aerodynamik. Göttingen 1927.

2. Bock, G.: Die gegenläufige Luftschraube und ihre Bedeutung für den Schnellflug. Jarhb.d.dtsch.Akad.d.Luftfahrtforschg. 1940/41 p.222.

3. Goldstein, S.: On the Vortex Theory of Screw Propellers. Proc. Roy. Soc. London (A) Vol. 123 (1929) p.440.

Lock, C. N., and Yeatman D.: Tables for the Use in an Improved Method of Airscrew Strip Theory Calculation. ARC - Rep. and Mem. 1674, 1935.

4. Glauert, H.: Grundlagen der Tragflügel- und Luftschraubentheorie. Berlin Springer 1929.

5. Helmbold, H. B.: Der Entwurf einer Luftschraube für gegebene Betriebsverhältnisse. Ringbuch der Luftfahrttechnik I C2.

6. Kramer, K. N.: Induzierte Wirkungsgrade von Bestluftschrauben endlicher Blattzahl Luftfahrt-Forschg. BD. 15 (1938). (Also available as NACA TM No. 884.) p. 320.

7. Kramer, K. N.: Ueber die Verbesserung des ideellen Wirkungsgrades bei Gegenlaufschrauben. FB 1558 (1941).

8. Kramer, K. N.: Ueber näherungsweise Luftschraubenrechnungen mittels Polaren. Jahrb. 1941 d. dtsch. Luftfahrt-forsch. p. I 404.

9. Lesley, E. P.: Tandem Air Propellers. NACA TN No. 689, 1939.

10. Lesley, E. P. and Reid, G. Elliot: Tests of Five Metal Model Propellers With Various Pitch Distributions.....
NACA TR No. 326, 1929.

11. Pistolesi, E.: Mutui influssi di eliche e di carene ed altri problemi sulle eliche. Aerotec. XXII Nr. 6.

12. Silber, R.: Sur l'interaction reciproque des helices d'un tandem tournant en sens inverse. C. R. Acad. Sci. Paris 21, 2,600 (1941).

13. Söhngen, H.: Angenäherte Berechnung der periodischen Luftkräfte an den Blattelementen von gegenläufigen Luftschrauben. FB 1222 (1940).

14. Walchner, O.: Berechnung der Eigenschaften einer Luftschraube von gegebener Form. Ringbuch der Luftfahrttechnik I C 7.

15. Walchner, O.: Berechnung von Luftschrauben mit kleinem Schubbeiwert und kleinem Fortschrittsgrad (Hubschrauben) Luftfahrtforschg. Bd. 13 (1936) p. 103

16. Weinig, F.: Aerodynamik der Luftschraube. Berlin, Springer 1940 p. 181.

COMPUTATION SHEET Ia (MULTISECTION METHOD)

$z = 2$ $\quad \boxed{x = 0.75}$ $\quad c_1 = \frac{8x}{\frac{z}{\pi}\frac{l}{R}} = 88.8$ $\quad c_{aI} = c_1 \kappa_I \sin \varphi_{w_I} \tan \alpha_{i_I}$ (equation 21) $\quad \lambda_I^* = x \tan(\varphi + \alpha_{II}^*)$

$\frac{l}{R} = 0.1061$ $\quad \lambda = 0.2865$ $\quad c_2 = \frac{z}{\pi}\frac{l}{R}\frac{1}{\lambda^2}\frac{1}{2x} = 0.549$ $\quad c_{aI}' = c_2\left(x^2 + \lambda_I^{*2}\right) c_{aI} \cos^2\alpha_{iI} \cos \varphi_{w_I}$ (equation 24) $\quad \lambda_{II}^* = x \tan(\varphi + \alpha_I^*)$

$\frac{d}{l} = 0.0785$ $\quad \overline{nb} = 2.62$ $\quad c_3 = \frac{z}{\pi}\frac{l}{R} = 0.06755$ $\quad \frac{dk_{aI}}{dx} = c_3\left(x^2 + \lambda_I^{*2}\right) c_{aI} \cos^2\alpha_{iI} \cos(\varphi_{w_I} + \gamma)/\cos\gamma$ (equation 22)

	Step 1 $\kappa_I = 0.612$	Step 2 $\kappa_I = 0.605$	Step 3				①	φ_{tI} / $\kappa_I\overline{w_{tI}}$	②	③	④	$\overline{w_{tII}}$		
β_d	0.4361						$\sqrt{6.864 - \frac{c_{aI}'}{\kappa_I}}$	2.62 - ①	$\kappa_I\overline{w_{tI}}(5.24 + \kappa_I\overline{w_{tI}}) - \frac{c_{aII}'}{\kappa_{II}}$	6.864 + ②	$\sqrt{③}$	④ - $\kappa_I\overline{w_{tI}}$ - 2.62	$\kappa_I\overline{w_{tI}} + \frac{\overline{w_{tII}}}{2}$	
$\varphi + \alpha_{II}^*$	.3649	0.3783	0.3775			Step 1	2.561	0.059 .0361	-0.1031	6.7609	2.600	-0.0561	0.00805	
$\beta_d - (\varphi + \alpha_{II}^*)$	.0712	.0577				Step 2	2.566	.054 .0327	-.1070	6.757	2.599	-.0537	.00585	
c_{aI}	.5695	.516												
$\cos^2\alpha_{iI}$	.999	.999			$\overline{w_{aI}}$	$\overline{w_{aII}}$	$\overline{w_{aI}}$	=	$\overline{w_{aII}}$	=	$\frac{z\bar{u}\,I}{\tan(\varphi + \alpha_{II}^*)}$		$\frac{z\bar{u}\,II}{\tan(\varphi + \alpha_I^*)}$	
$\cos\varphi_{w_I}$	.9240	.9198			$\frac{\overline{w_{tI}}}{\tan\varphi_{w_I}}$	$\frac{-\overline{w_{tII}}}{\tan\varphi_{w_{II}}}$	$\frac{\left(2.62 - \frac{\overline{w_{tI}}}{2}\right)\overline{w_{tI}}}{1 + \kappa_{II}\frac{\overline{w_{aII}}}{2} + \frac{\overline{w_{aI}}}{2}}$		$\frac{-\left(2.62 + \kappa_I\overline{w_{tI}} + \frac{\overline{w_{tII}}}{2}\right)\overline{w_{tII}}}{1 + k_I\frac{\overline{w_{aI}}}{2} + \frac{\overline{w_{aII}}}{2}}$		$\frac{1 + k_{II}\frac{\overline{w_{aII}}}{2}}{2.62}$		$\frac{1 + \kappa_I\frac{\overline{w_{aI}}}{2}}{2.62 + \kappa_I\overline{w_{tI}}}$	
$\cos(\varphi_{w_I} + \gamma)/\cos\gamma$ $\tan(\varphi_{w_I} + \gamma)$		.9077 .4623		Step 1	0.1426	0.1360	$\frac{2.590 \times 0.059}{1.112} = 0.1375$		$\frac{2.656 \times 0.0561}{1.1101} = 0.1339$		$\frac{1.041}{2.62}$	= 0.3975	$\frac{1.042}{2.656}$	= 0.3925
c_{aI}'	.1860	.1693		Step 2	.1266	.1275	$\frac{2.593 \times 0.054}{1.1027} = 0.1270$		$\frac{2.653 \times 0.0537}{1.1031} = 0.1293$		$\frac{1.039}{2.62}$	= 0.3965	$\frac{1.038}{2.653}$	= 0.3915
c_{aI}'/κ_I c_a'	.304	.2800 .3383												
$\frac{\overline{v}_1}{1 + \frac{\kappa_I\overline{w_{aI}} + \kappa_{II}\overline{w_{aII}}}{2}}$		1.078 1.077												
dk_{aI}/dx dk_{lI}/dx		.02056 .00714	$\frac{dk_a}{dx} = 0.04104$ $\frac{dk_l}{dx} = 0.01416$											

COMPUTATION SHEET Ib

$\boxed{x = 0.75}$

$\lambda = 0.2865$

$c_l = 88.8$	α_d	$\varphi_w = \beta_d - \alpha_d$	$\alpha_i = \beta_d - \left(\varphi + \alpha_{II}^*\right) - \alpha_d$	$\sin \varphi_w$	$\tan \alpha_i$	c_a		$5.38\alpha_d + 0.337$	
$\kappa_I c_l = 54.35$	0.03	0.4061	0.0412	0.3950	0.0412	0.884		0.499	
Step 1	.05	.3861	.0212	.3766	.0212	.434		.602	
	.0438	.3923	.0274	.3823	.0274	.5695		.573	
$\kappa_I c_l = 53.75$	.033	.4031	.0247	.3923	.0247	.520		.514	
Step 2	.0332	.4029	.0245	.3921	.0245	.516		.516	

COMPUTATION SHEET IIa

$x = 0.75$

$\lambda = 0.2865$

	Step 1	Step 2	Step 3
	$k_{II} = 0.612$	$k_{II} = 0.605$	
β_d	0.4311		
$\varphi + \alpha_I^*$	.3649	0.3740	0.3732
$\beta_d - (\varphi + \alpha_I^*)$	.0662	.0571	
c_{aII}	.5495	.5150	
$\cos^2\alpha_{iII}$	.999	.999	
$\cos \varphi_{wII}$	.9244	.9215	
$\cos(\varphi_{wII} + \gamma)/\cos\gamma$ $\tan(\varphi_{wII} + \gamma)$		.9094 .4574	
c_{sII}'	.1796	.1690	
c_{sII}'/κ_{II}	.2935	.2794	
$\frac{dk_{sII}}{dx}$		.02048	
$\frac{dk_{lII}}{dx}$		.00702	

COMPUTATION SHEET IIb

$\boxed{x = 0.75}$

$\lambda = 0.2865$

	$c_l = 88.8$	α_d	$\varphi_w = \beta_d - \alpha_d$	$\alpha_l = \beta_d - (\varphi + \alpha_T^*) - \alpha_d$	$\sin \varphi_w$	$\tan \alpha_l$	c_a		$5.38\alpha_d + 0.337$	
Step 1	$\kappa_{II} c_l = 54.35$	0.04	0.3911	0.0262	0.3812	0.0262	0.543		0.552	
		.0398	.3913	.0265	.3814	.0265	.5495		.551	
Step 2	$\kappa_{II} c_l = 53.75$	.033	.3981	.0241	.3877	.0241	.502		.515	
		.0326	.3985	.0245	.3880	.0245	.511		.518	
		.0322	.3989	.0249	.3884	.0249	.520		.510	
		.0324	.3987	.0247	.3882	.0247	.515		.511	

COMPUTATION SHEET IIIa (SINGLE SECTION METHOD)

$z = 2$ $\quad \lambda = 0.573$

$\tau_\sigma = l_\sigma/D = 0.0566$ $\quad \overline{\kappa w} = 1.222$

$\vartheta_\sigma = d_\sigma/l_\sigma = 0.0829$

1	λ_I^*	Step 1 0.573	Step 2 0.582				①	$\frac{\overline{w_{tI}}}{\kappa_I \overline{w_{tI}}}$	②	③	④	$\overline{w_{tII}}$	
2 3	$\tan \varphi_{\sigma I}^* = \lambda^*/0.7$ $\varphi_{\sigma I}^* = \arctan$ ②	.819 .686	.832 .694				$\sqrt{1.492 - \frac{c_{aI}'}{\kappa_I}}$	1.222 - ①	$\kappa_I \overline{w_{tI}}\left(2.444 + \kappa_I \overline{w_{tI}}\right) - c_{aII}'/\kappa_{II}$	1.492 + ②	$\sqrt{③}$	④ - $\kappa_I \overline{w_{tI}}$ - 1.222	$\kappa_I \overline{w_{tI}} + \frac{\overline{w_{tII}}}{2}$
4 9	$\sigma^2 + \lambda_I^{*2} = 0.49 + ①^2$ $\beta_{d\sigma I}$	.818 .805	.828 .805			Step 1	1.152	0.070 .0322	-0.0618	1.430	1.196	-0.058	0.003
10 11	$\vartheta_\sigma = z/\pi\sigma$ $\alpha_{dI} + \alpha_{1I} = \beta_{dI} - \varphi_I^* =$ ⑨ - ③	.0360 .119	.0360 .111			Step 2	1.155	.067 .0306	-.0710	1.421	1.193	-.060	.001
12 13	α_{1I1} $f_{\sigma I1}$ with $\varphi_{wI} =$ ③ + ⑫	.036 .852	.036 .859										
14 15	$c_{aI1} = \frac{⑬ \tan ⑫}{⑩}$ α_{1I2}	.852	.859 .030										
16 17	$f_{\sigma I2}$ $c_{aI2} = \frac{⑯ \tan ⑮}{⑩}$		.846 .705		w_{aI}	w_{aII}	$w_{aI} =$		w_{aII}		$\frac{z\kappa I}{\tan\left(\varphi_\sigma + \alpha_I^*\right)}$		$\frac{z\kappa II}{\tan\left(\varphi_\sigma + \alpha_I^*\right)}$
18 19	α_{1I} α_{dI}	.036 .086	.033 .0775		$\frac{\overline{w_{tI}}}{\tan \varphi_{wI}}$	$\frac{\overline{w_{tII}}}{\tan \varphi_{wII}}$	$\frac{\left(1.222 - \frac{\overline{w_{tI}}}{2}\right)\overline{w_{tI}}}{1 + k_{II}\frac{\overline{w_{aII}}}{2} + \frac{\overline{w_{aI}}}{2}}$		$\frac{-\left(1.222 + \kappa_I \overline{w_{tI}} + \frac{\overline{w_{tII}}}{2}\right)\overline{w_{tII}}}{1 + \kappa_I \frac{\overline{w_{aI}}}{2} + \frac{\overline{w_{aII}}}{2}}$	$\frac{1 + \kappa_{II}\frac{\overline{w_{aII}}}{2}}{1.222}$			$\frac{1 + \kappa_I \frac{\overline{w_{aI}}}{2}}{1.222 + \kappa_I \overline{w_{tI}}}$
20 21	c_{aI} c_{w_I} with $\vartheta_{\sigma I}$ ⑧, ⑳	.850 .060	.800 .059	Step 1	0.0795	0.0680	$\frac{1.187 \times 0.070}{1.056} = 0.0787$		$\frac{1.225 \times 0.058}{1.050} = 0.0665$		0.832		0.812
22 23	$\varepsilon_I =$ ㉑ / ⑳ $\gamma_I =$ arc tan ㉒	.071 .071	.074 .074	Step 2	.0758	.0696	$\frac{1.189 \times 0.067}{1.054} = 0.0756$		$\frac{1.223 \times 0.060}{1.052} = 0.0698$		.832		.811
24 25	$\cos^2\alpha_{1I}/\cos\gamma_I$ $\varphi_I^* + \alpha_{1I} + \gamma_I =$ ③ + ⑱ + ㉓	1.- 1.-	1.- .801										
26 27	$\tan\left(\varphi_I^* + \alpha_{1I} + \gamma_I\right) = \tan$ ㉕ $\sin\left(\varphi_I^* + \alpha_{1I} + \gamma_I\right) = \sin$ ㉕		1.032 .718										
28 29	$\eta_I =$ ② / ㉖ $= \frac{\tan \varphi_\sigma}{㉖}$ $k_{1I} = \frac{④ ⑩ ⑳ ㉗ ㉔}{1.273}$	.791 .0146	.794 .01348	$k_t = 0.02607$		φ_{wI} λ_{1I}	0.722 .616	0.730 .626	0.724 .619				
30 31	$k_{aI} =$ ㉘ ㉙ / ① $= \frac{㉘ ㉙}{\lambda}$ $c_{a_I} =$ ㉚ $/\lambda^2$	.0196 .0598	.01865 .0568	$k_a = 0.03647$		κ $f_\sigma = 2.8\kappa \sin \varphi_w$	.46 .852	.46 .859	.456 .846				
32	$c_{aI}' = 1.273$ ㉛ c_{aI}'/κ_I	.0761 .1655	.0724 .1588										

Computation Sheet IIIb

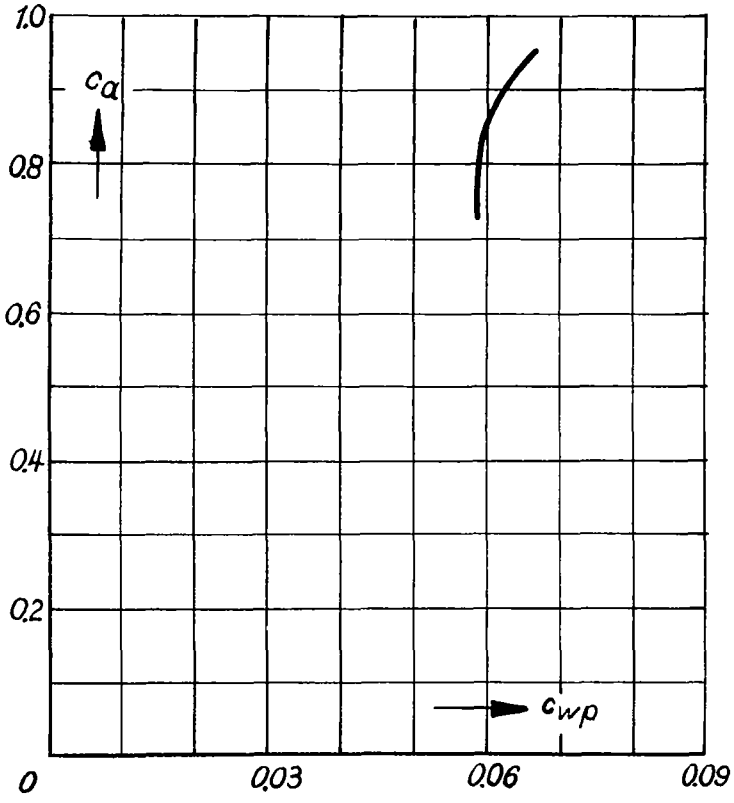

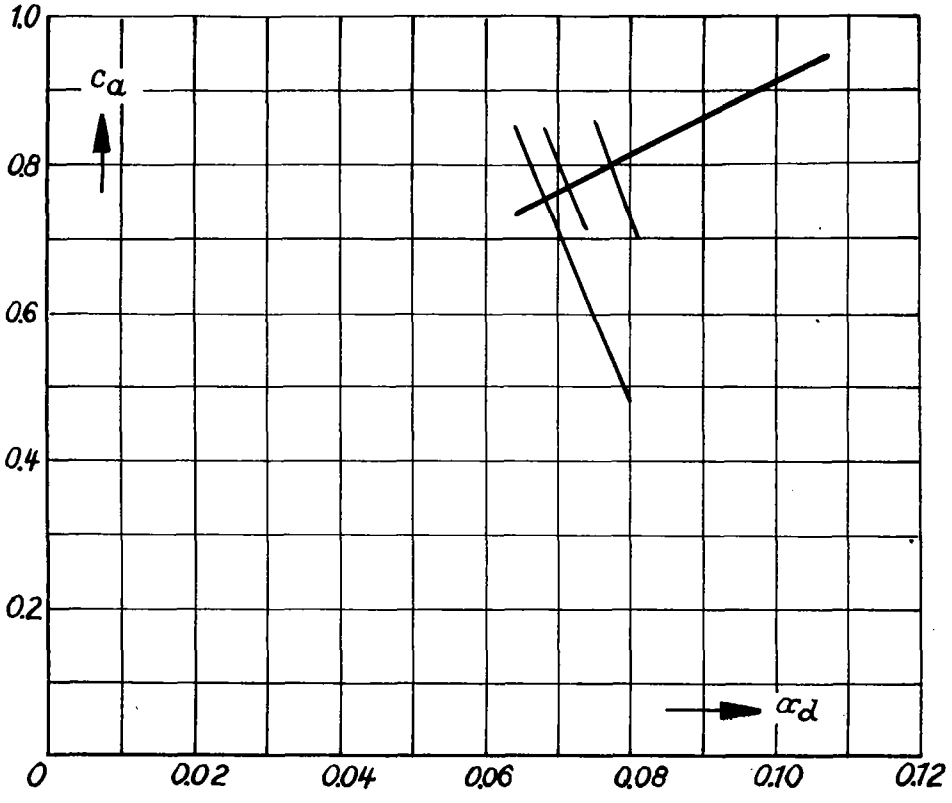

COMPUTATION SHEET IV

$\lambda = 0.573 \qquad \frac{xp}{v} = 1.222$

1	λ_{II}^*	Step 1 0.573	Step 2 0.568					
2	$\tan \varphi_{\sigma II}^* = \lambda^*/0.7$	.819	.812					
3	$\varphi_{\sigma II}^* = \text{arc tan } ②$	.686	.682					
4	$\sigma^2 + \lambda_{II}^{*2} = 0.49 + ①^2$	.818	.812					
9	$\beta_{d\sigma II}$	.786	.786					
10	$\delta_\sigma = z/\pi\tau_\sigma$	.0360	.0360					
11	$\alpha_{d_{II}} + \alpha_{iII} = \beta_{d_{II}} - \varphi_{II}^* = ⑨ - ③$	.100	.104					
12	α_{iIII}	.036	.036					
13	$f_{\sigma_{III}}$ with $\varphi_{wII} = ③ + ⑫$	.852	.852					
14	$c_{a_{III}} = \frac{⑬ \tan ⑫}{⑩}$	.852	.852					
15	α_{iII2}	.020	.030					
16	$f_{\sigma II2}$	.863	.858					
17	$c_{aII2} = \frac{⑯ \tan ⑮}{⑩}$	.479	.715					
18	α_{iII}	.032	.032					
19	α_{dII}	.068	.0715					
20	c_{aII}	.752	.770					
21	$c_{w_{II}}$ with $\delta_{\sigma_1} ⑧ ⑳$	.0615	.0603					
22	$\epsilon_{II} = ㉑/⑳$	.0818	.0784					
23	$\gamma_{II} = \text{arc tan } ㉒$	.0816	.0782					
24	$\cos^2\alpha_{iII}/\cos \gamma_{II}$	1.0	1.0					
25	$\varphi_{II}^* + \alpha_{iII} + \gamma_{II} = ③ + ⑱ + ㉓$	.800	.792					
26	$\tan(\varphi_{II}^* + \alpha_{iII} + \gamma_{II}) = \tan ㉕$	1.030	1.013	φ_{wI}	0.722	0.706	0.718	0.712
27	$\sin(\varphi_{II}^* + \alpha_{iII} + \gamma_{II}) = \sin ㉕$	.717	.712	λ_{iI}	.616	.597	.612	.604
28	$\eta_{II} = ②/㉖ = \frac{\tan f_\sigma}{㉖}$	.795	.809	κ	.46	.475	.462	.470
29	$k_{iII} = \frac{④ ⑩ ⑳ ㉗ ㉔}{1.273}$	.01245	.01259	$f_\sigma = 2.8_\kappa \sin \varphi_w$	.852	.863	.852	.858
30	$k_{aII} = ㉘ ㉙/① = \frac{㉘ ㉙}{\lambda}$	.0173	.01777					
31	$c_{aII} = ㉚/\lambda^2$	.0528	.0542					
32	$c_{aII}' = 1.273 ㉛$	.0672	.0690					
	c_{aII}'/κ_{II}	.1415	.1467					

TABLE 1.- COMPARISON OF TOTAL VALUES BETWEEN CALCULATION AND MEASUREMENT

	Calculation						Measurement		
	$\beta_{dI0.75}$	λ	k_s	k_ζ	η		k_s	k_ζ	η
Counterrotating propeller with 2 × 2 blades	25°	0.2	0.036	0.0097	0.73	Multisection method	0.039	0.0109	0.73
	25°	.3	.017	.0058	.86		.020	.0075	.82
	45°	.573	.036	.026	.80	Single section method	.038	.027	.81
4-blade propeller	25°	.2	.035	.0096	.72	Multisection method	.037	.0104	.72
	25°	.3	.017	.0060	.85		.019	.0073	.80

TABLE 2.- VERIFICATION OF THE CALCULATION

$\lambda = 0.2$ $\lambda = 0.3$ $\lambda = \frac{0.9}{\pi}$ $\lambda = \frac{0.9}{\pi}$

with $\beta_I - \beta_{II}$ according to equation (44)

$k_{lI} = k_{lII}$

x = 0.30	$\frac{dk_{sI}}{dx}$	0.0063	0.00025		
	$\frac{dk_{sII}}{dx}$	.0066	.00008		
	$\frac{dk_{lI}}{dx}$	.00156	.000080		
	$\frac{dk_{lII}}{dx}$	.00159	.000025		
x = 0.45	$\frac{dk_{sI}}{dx}$	.0163	.0062	0.0077	0.0077
	$\frac{dk_{sII}}{dx}$	.0173	.0065	.0080	.0082
	$\frac{dk_{lI}}{dx}$	.0044	.0022	.00261	.00261
	$\frac{dk_{lII}}{dx}$	.0044	.0023	.00265	.00270
x = 0.60	$\frac{dk_{sI}}{dx}$	.0273	.0134		
	$\frac{dk_{sII}}{dx}$	.0278	.0138		
	$\frac{dk_{lI}}{dx}$	.0076	.00470		
	$\frac{dk_{lII}}{dx}$	.0075	.0048		
x = 0.75	$\frac{dk_{sI}}{dx}$	.0343	.0183	.0206	.0204
	$\frac{dk_{sII}}{dx}$	.0343	.0180	.0205	.0206
	$\frac{dk_{lI}}{dx}$	.0097	.00659	.00714	.0707
	$\frac{dk_{lII}}{dx}$	.0093	.00639	.00702	.00706
x = 0.90	$\frac{dk_{sI}}{dx}$	.0326	.0183	.0203	
	$\frac{dk_{sII}}{dx}$	.0320	.0181	.0197	
	$\frac{dk_{lI}}{dx}$	.0093	.0068	.0072	
	$\frac{dk_{lII}}{dx}$	.0091	.0066	.0069	

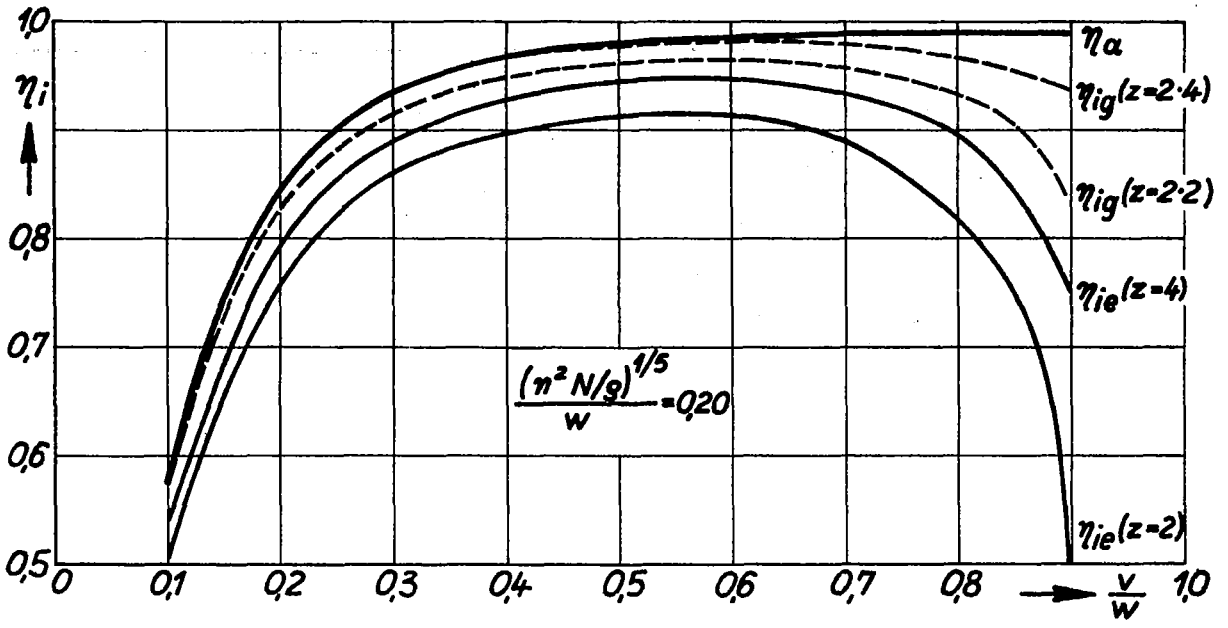

Figure 1.- Efficiencies as functions of the relation flight velocity/tip velocity.

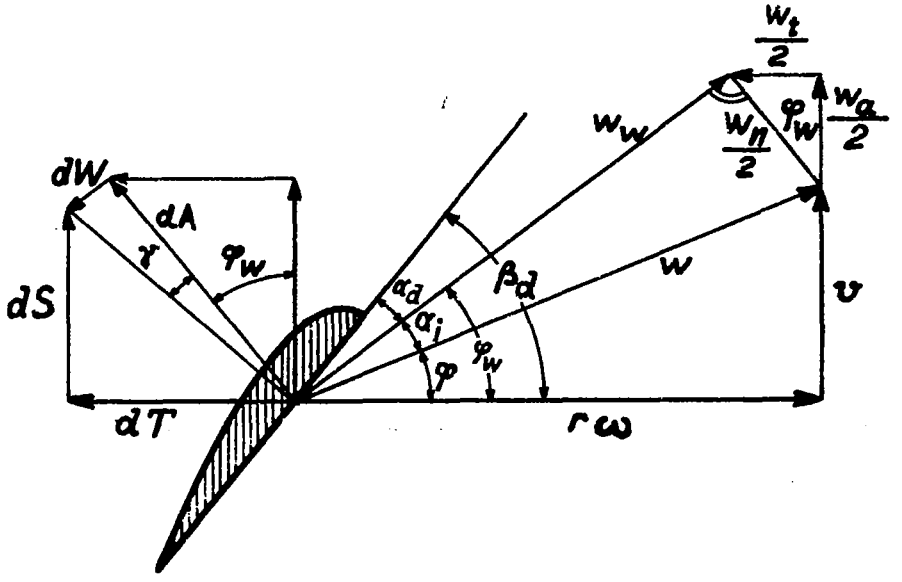

Figure 2.- Velocity plan and force plan for the element of the single propeller in undisturbed flow.

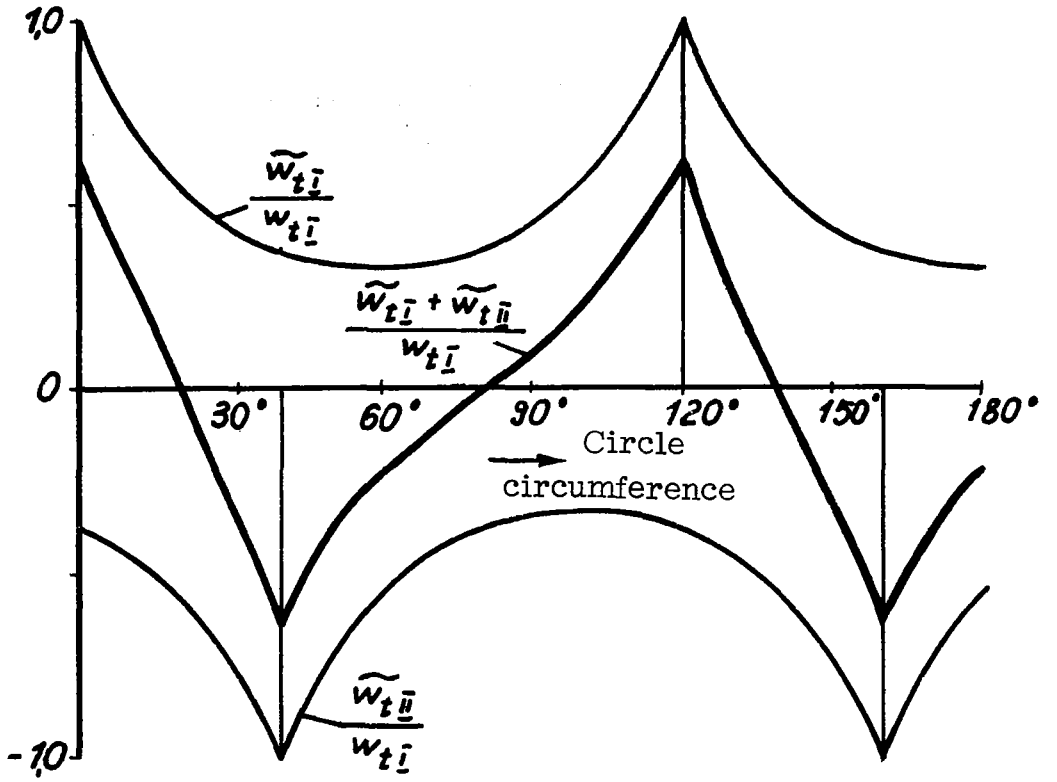

Figure 3.- Variation of the induced tangential velocities far behind the single and the counter-rotating propeller along a circle around the slipstream axis for z = 3 (from [7]).

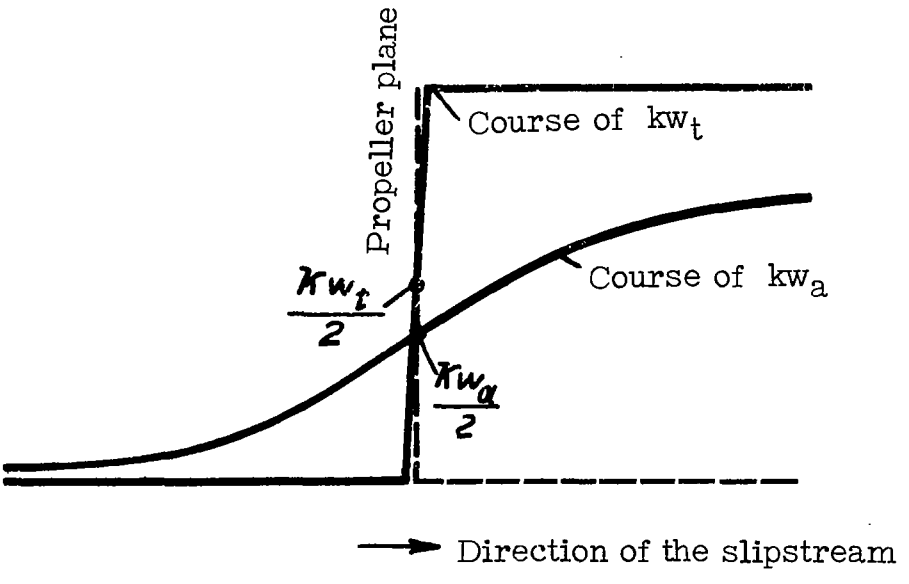

Figure 4.- Variation of the induced mean velocities in the direction of the slipstream.

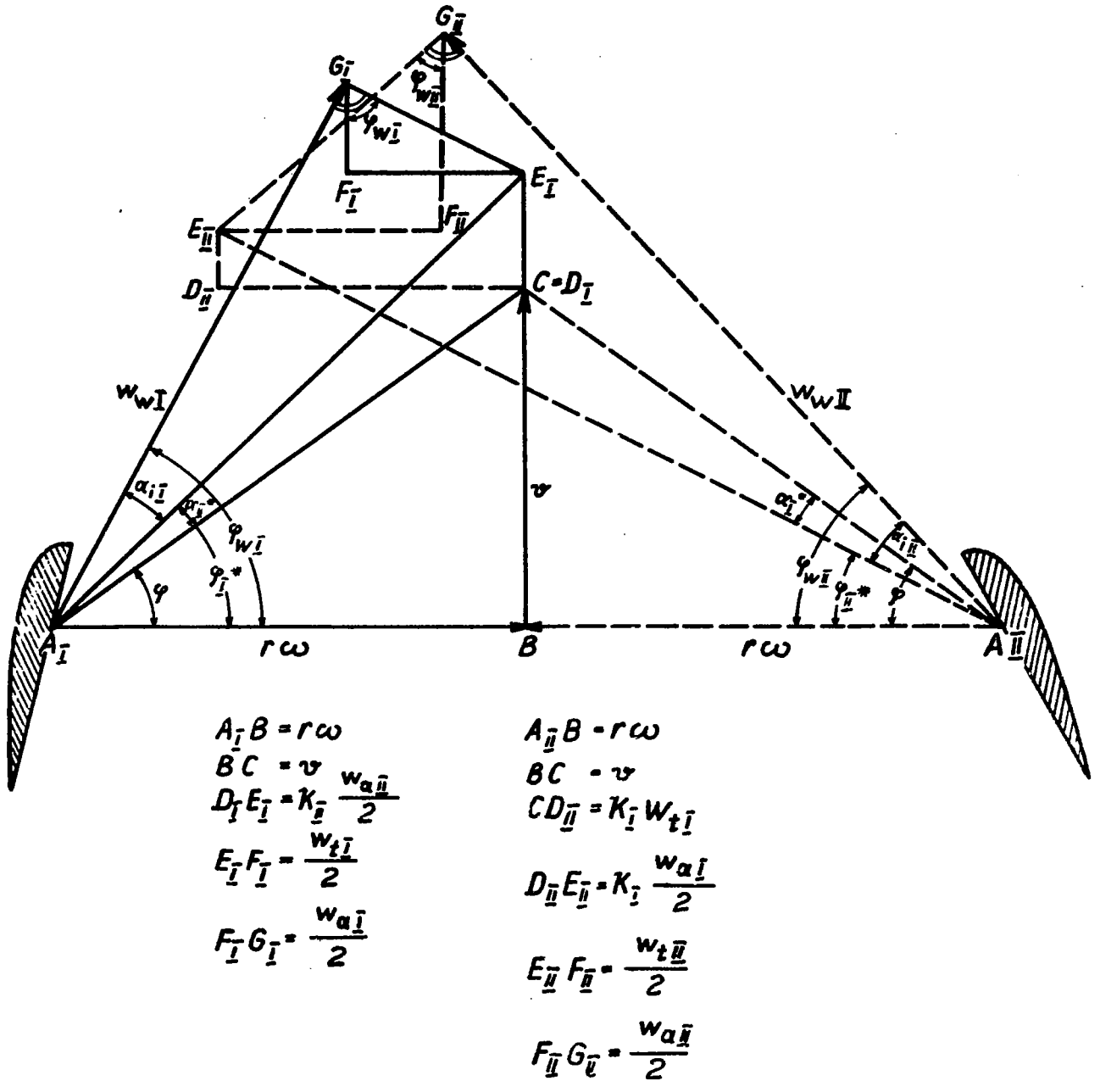

Figure 5.- Velocity plan for the counter-rotating propeller (according to [7]).

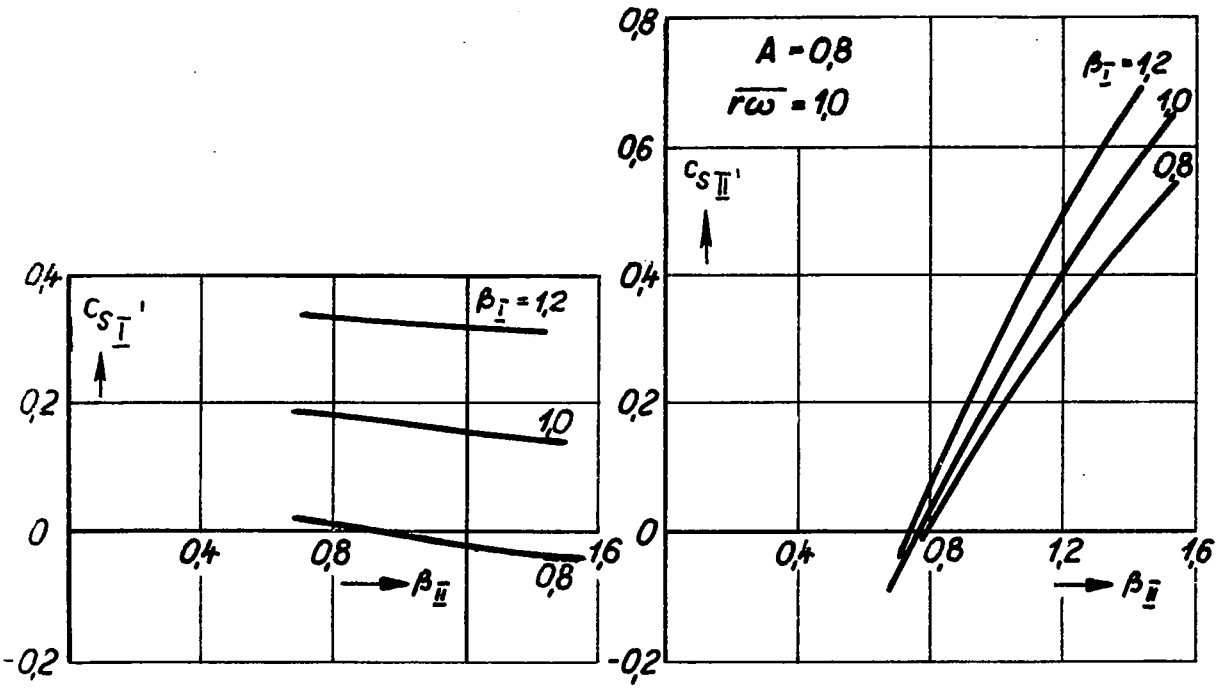

Figure 6.

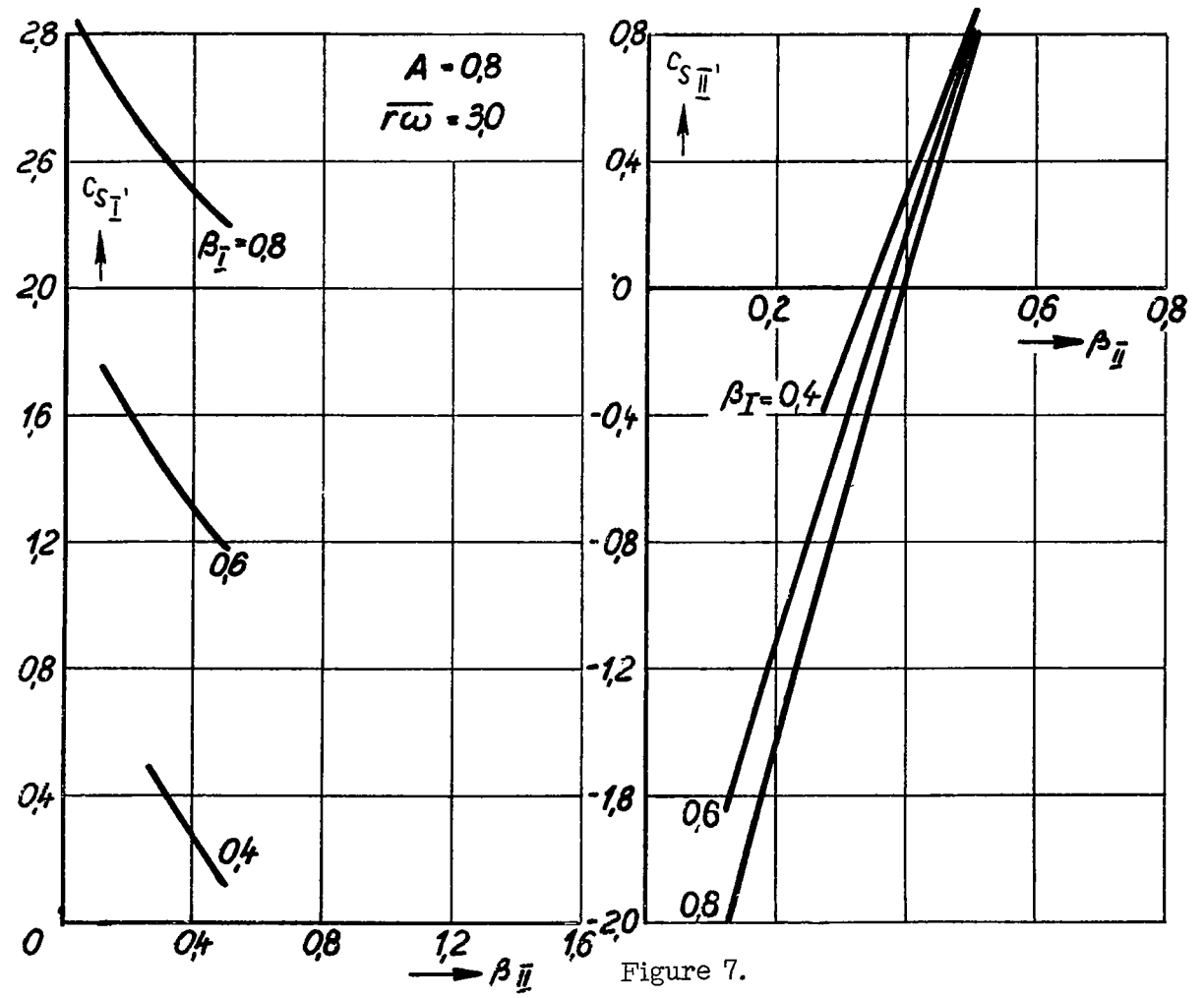

Figure 7.

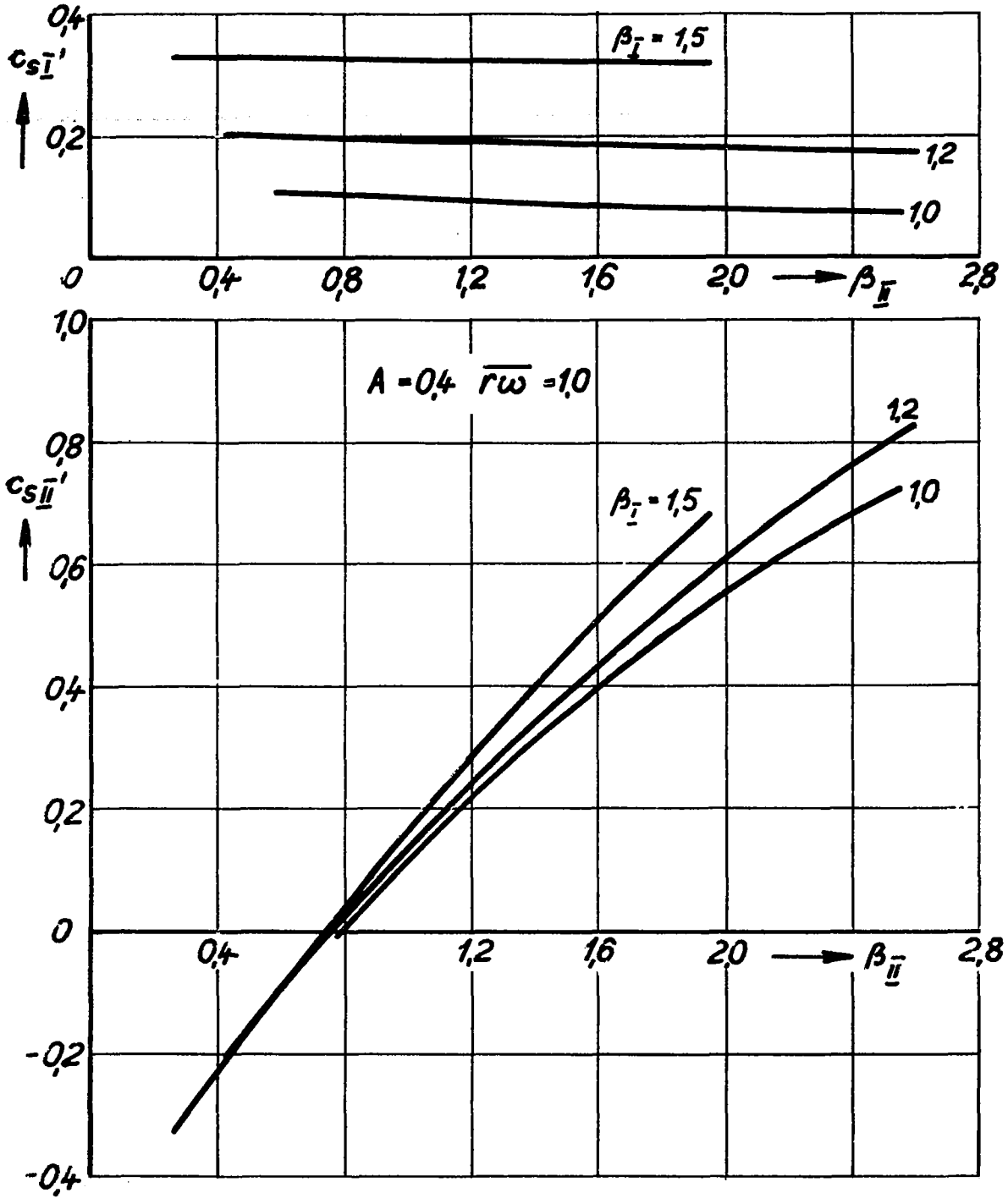

Figures 6 to 8.- Examples for the dependence of the local thrust loadings of the counter-rotating propeller with an infinite number of blades on the blade angles of the two partners, on the form parameter $A = \frac{l}{2\pi r} \frac{dc_a}{d\alpha} z$ and on $\frac{r\omega}{v}$.

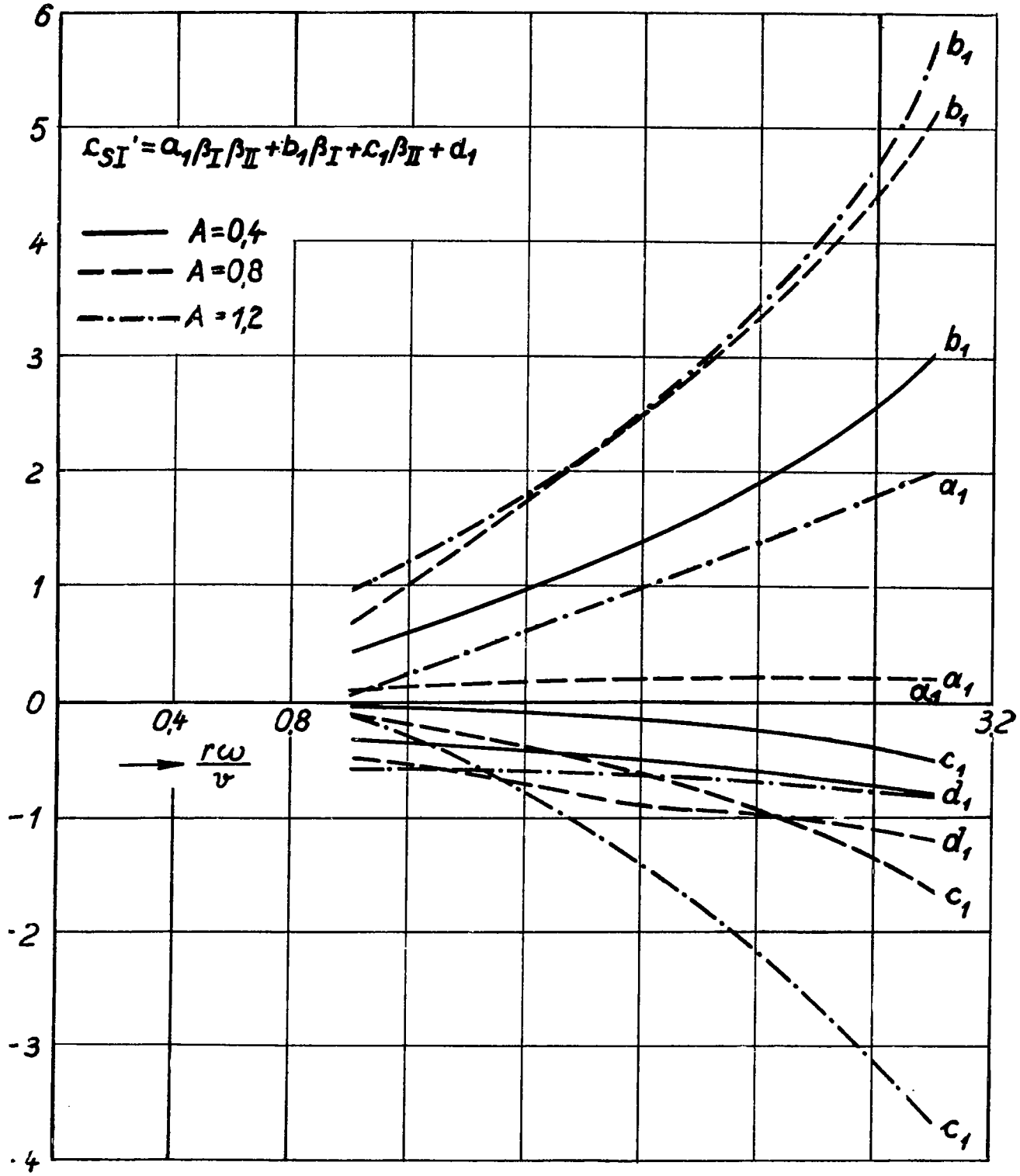
$c_{SI}' = a_1\beta_I\beta_{II} + b_1\beta_I + c_1\beta_{II} + d_1$
A=0,4
A=0,8
A=1,2
6
5
4
3
2
1
0
-1
-2
-3
-4
0,4
0,8
3,2
$\frac{r\omega}{v}$
b_1
b_1
b_1
a_1
a_1
a_1
c_1
d_1
d_1
c_1
c_1

Figure 9.

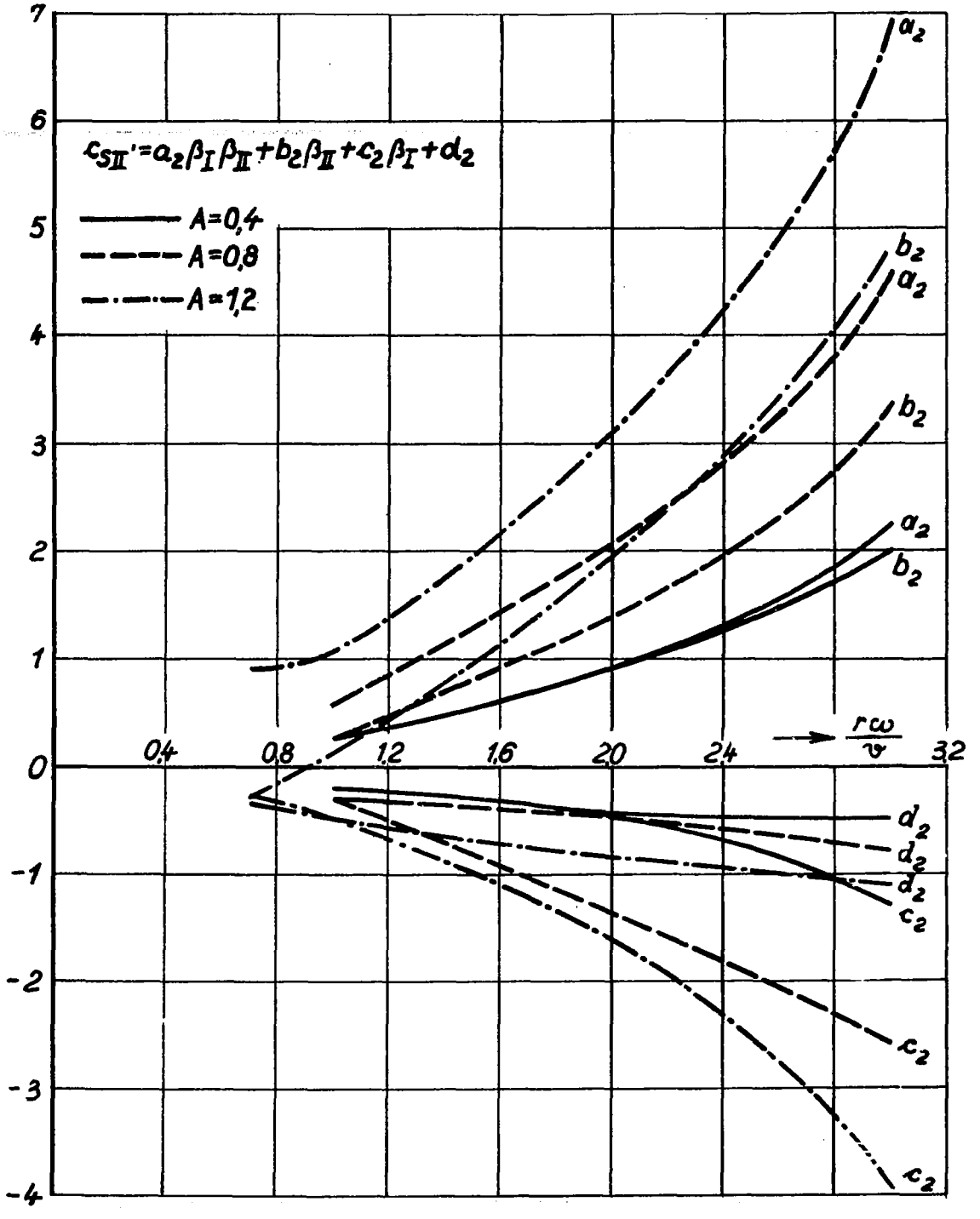

Figures 9 and 10.- Coefficients of the interpolation formulas for the local thrust loading as a function of $\frac{r\omega}{v}$ and of the form parameter $A = \frac{l}{2\pi r} \frac{dc_a}{d\alpha} z$.